AC SAF VALIDATION REPORT

Validated product:

Identifier	Name	Acronym
O3M-88	Level-3 Total H_2O Data Record from GOME-2A&B	MXG-DS-TCDRH2O

GOME-2/MetOp-A in April 2013

Authors:

Name	Institute
Pieter Valks	German Aerospace Center
Margherita Grossi	German Aerospace Center
Sander Slijkhuis	German Aerospace Center
Marc Schröder	Deutscher Wetterdienst
Heidrun Höschen	Deutscher Wetterdienst

Document Change Record

Document, Version	Date	Changes	Originator
1.0	2017.06.06	Original version	P. Valks, M. Grossi, M. Schröder, H. Höschen
1.1	2017.11.06	Several updates after DRR	S. Slijkhuis, P. Valks

Table of Contents

1 Introduction

1.1 Purpose and scope

This report presents the results of the complementary validation of the GOME-2 H_2O level 3 climate product (O3M-88) with ground based and SSM/I water vapour observations. The validation has been carried out by the AC SAF (formerly known as O3M SAF) and the CM SAF in the framework of a SAF Federated Activity.

1.2 Background and introduction

The knowledge of the effective distribution of the total column water vapour (TCWV) in the atmosphere is fundamental for weather monitoring as well as for the evaluation of climate models. Advancing in understanding of variability and changes in water vapor is vital, especially considering that, in contrast to most other greenhouse gases, the H_2O distribution is highly variable.

A level 3 TCWV data record (O3M-88) from GOME-2 observations has been produced by the AC SAF in the CDOP-2. The monthly level 3 TCWV data have been generated with consolidated algorithms applied in a consistent way to a homogeneous (reprocessed) GOME-2 FCDR level-1 data-set from both MetOp-A and -B.

In order to assess the quality of the GOME-2 level 3 TCWV data, a complementary validation with ground based and SSM/I observations has been performed. Comparisons with TCWV data from the Global Navigation Satellite System GNSS data base and GCOS Reference Upper Air Network (GRUAN) radiosondes have been made. Furthermore, the GOME-2 TCWV data have been compared to the CM SAF data set (CM-12701) derived from Special Sensor Microwave/Imager (SSM/I) and Special Sensor Microwave Imager Sounder (SSMIS) observations on-board polar orbiting satellites (DMSP). Note that for the validation of the Level-2 GOME-2 H2O column product, a more extensive validation has been carried out, as described in the corresponding AC SAF validation report (Grossi et al., 2015) and AMT papers (Grossi et al., 2015; Kalokoski et al., 2016). These validation exercises also included comparisons with MERIS satellite data over land.

1.3 Structure of the document

The structure of this report is as follows:

The main validation results are summarized in Sect. 2. The validation report of the GOME-2 Level 3 TCWV data record with HOAPS-4 SSM/I observations is provided in Annex 3.1 on page 8. The validation results with NCAR GNSS and GRUAN ground-based data are reported in Annex 3.2 on page 29.

2   Executive Summary

In the CDOP-2, a level 3 TCWV data record from GOME-2 observations has been produced by the AC SAF. The gridded product contains monthly mean TCWV data on a regular 0.5°x0.5° longitude/latitude grid in netCDF-4 format, and includes support data related to clouds and surface properties. The GOME-2 TCWV product covers the period January 2007 to December 2015 (for GOME-2/MetOp-A) and January 2013 to December 2015 (for GOME-2/MetOp-B).

The GOME-2 TCWV data have been compared with ground based and HOAPS-4 SSM/I observations, and the quality of the GOME-2 water vapour data has been assessed. In general, the results presented in the two validation reports (see Annex 3) show that the GOME-2 level-3 TCWV product usually fulfills the user requirements in terms of target (10%) accuracy stated in the AC SAF Product Requirements Document (PRD).

The main results of the validation of the GOME-2 level-3 TCWV data record with HOAPS-4 SSM/I observations from the CM SAF are:

- The HOAPS-4 TCWV data record was retrieved with a newly developed 1D-Var scheme and the product is based on SSM/I and SSMIS observations. The product consist of monthly means on a regular 0.5°x0.5° longitude/latitude grid and covers the period July 1987 – December 2014.

- Global comparison between the GOME-2 and the SSM/I products.

  When averaged over the overlap period January 2007 to December 2014, it was found that the mean bias w.r.t. the SSM/I observations is small and negative (-0.7 kg/m^2 for the comparison with GOME-2A and -0.3 kg/m^2 for the comparison with GOME-2B) and the product fulfils the requirements in term of optimal accuracy (5%) stated by AC SAF PDR.

- Monthly comparison between the GOME-2 and the SSM/I products.

  The comparison revealed a strong seasonal cycle in the distribution of the bias, with larger positive values in the northern hemisphere summer months and lower negative values in the northern hemisphere winter months. The amplitude of the summer winter oscillations was large (up to 1.7 kg/m^2), and the discrepancies were mainly associated to residual cloud contamination. Also, larger bias was observed over ocean and over land areas with high humidity and a relatively large surface albedo, as already reported in a previous validation study of the operational GOME-2 level 2 TCWV product provided by the AC SAF.

The results of the comparison between the GOME-2 level 3 TCWV product and the SSM/I data from the CM SAF have been discussed in details in the AC SAF validation report in Annex 3.1 on page 8.

The main results of the validation of the GOME-2 level-3 TCWV data record with NCAR GNSS and GRUAN ground-based data are:

- The availability and applicability of ground-based observations of TCWV such as from ARM (microwave radiometer), NDACC (lidar) and GRUAN (radiosondes) networks was assessed. In agreement with AC SAF it was decided to utilise TCWV data from NCAR GNSS and GRUAN radiosondes as references.

- The comparison with GNSS reveals that the global mean bias is -0.56 kg/m^2 (0.4 kg/m^2) while the RMS is 4.76 kg/m^2 (5.42 kg/m^2) for GOME-2A (GOME-2B). For GOME-2A the relative difference occasionally exceeds 10%. The seasonal analysis exhibits that the absolute bias is largest/smallest in summer/fall. The RMS exhibits a seasonal cycle with maximum/minimum values in summer/winter. The global distribution of bias and RMS appears mainly random, except from larger values at coastal stations and a slight tendency for larger values in the tropics (bias and RMS) and a slight zonal dependence (RMS).

Results related to the use of GRUAN data as reference supports the features found in the comparison with GNSS. However, comparing GOME-2 to GRUAN reveals a negative bias for GOME-2A and for GOME-2B, with a comparable difference in bias between the two satellites though. Note that less data was included and therefore some investigations done for GNSS are not adequate for a comparison with GRUAN and are not shown here.

Thus, a discontinuity between GOME-2A and GOME-2B seems to be evident, but the effect is smaller than 1 kg/m^2.

The results of the comparison between the GOME-2 level 3 TCWV product and the NCAR GNSS and GRUAN ground-based data have been discussed in detail in the CM SAF validation report in Annex 3.2 on page 29.

3   Annex

		Ref:	SAF/AC/DLR/VR/L3_H2O			
		Date:	06 November 2017			
		Issue:	1	Revision:	1	Page 8

EUMETSAT
AC SAF
ATMOSPHERIC COMPOSITION MONITORING

Annex 3.1: Validation of GOME-2 Level 3 TCWV data record with SSM/I observations (AC SAF report)

Product Validation Report
GOME-2 vs. HOAPS4 SSM/I

Validated products:

Identifier	Name
O3M-88	TCWV Level-3 product from GOME-2
CM-12701	TCWV Level-3 product from SSM/I+SSMIS

Reference Number: **SAF/O3M/DLR/FA/GOME-2**

Issue/Revision Index: **1.0**

Date: **24.01.2017**

Report Change Record

Report Version	Date	Changes	Originator
1.0	2017.01.24	Original version	M. Grossi
1.1	2017.11.10	Several updates after DRR	S. Slijkhuis, P. Valks

1 Introduction

1.1 Purpose

The purpose of this report is to present the results of the comparison of monthly Total Column Water Vapor (TCWV) measurements from the ultraviolet spectrometer Global Ozone Monitoring Experiment-2 (GOME-2) on METOP-A and METOP-B and the CM SAF data set derived from Special Sensor Microwave/Imager (SSM/I) and Special Sensor Microwave Imager Sounder (SSMIS) observations on-board polar orbiting satellites (DMSP). The most recent version of the Hamburg Ocean-Atmosphere Parameters and Fluxes from Satellite (HOAPS) algorithm (HOAPS-4.0) has been used to produce monthly means gridded dataset from the SSM/I and SSMIS passive microwave radiometers. For the generation of the L3 GOME-2 monthly gridded product, the Level 2 reprocessed GOME-2 H_2O column data generated by DLR using the GOME Data Processor (GDP) version 4.8 are used.

The overall consistency between measurements from the GOME-2 instruments and the CM SAF total column water vapour (WVPA) data set is evaluated in the overlap period January 2007 to December 2014. It is important to assess the accuracy and improve the post processing of satellite data in order to have a consistent picture of the coherence of the results produced employing different technologies.

This comparison is carried out within a Federated Activity between AC SAF and CM SAF during CDOP2. Objectives of the FA are the complementary validation of GOME-2 TCWV Level 3 data using ground-based and SSM/I observations and the co-operation on validation of total column water vapour (TCWV) data sets from AC SAF and CM SAF.

1.2 Definitions, acronyms and abbreviations

AMF	Air Mass Factor
CM SAF	EUMETSAT Satellite Application Facility on Climate Monitoring
DOAS	Differential Optical Absorption Spectroscopy
EUMETSAT	European Organisation for the Exploitation of Meteorological Satellites
GCOS	Global Climate Observing System
GOME-2	Global Ozone Monitoring Experiment-2
GOME-2A	GOME-2/MetOp-A
GOME-2B	GOME-2/MetOp-B
H_2O	Water Vapour
HOAPS	Hamburg Ocean-Atmosphere Parameters and Fluxes from Satellite
METOP	Meteorological Operational Satellite
REMSS	Remote Sensing System
RMS	Root Mean Square Error
SSM/I	Special Sensor Microwave/Imager
SSMIS	Special Sensor Microwave Imager Sounder
TCWV	Total Column Water Vapor
UPAS	Universal Processor for UV/VIS Atmospheric Spectrometers

VCD   Vertical Column Density

1.3 Applicable documents

[AD-1]   **ATBD** Algorithm Theoretical Basis Document for GOME-2 Total Column Products of Ozone, NO2 , SO2, BrO, H2O, HCHO and Cloud Properties, DLR/GOME-2/ATBD/01, Rev. 3/A, P. Valks et al., October 2016.

[AD-2]   **PUM** Product User Manual for GOME-2 Total Columns of Ozone, NO2, SO2, BrO, H2O, HCHO, and Cloud Properties, DLR/GOME-2/PUM/01, Rev. 3/A, Valks, et. al., October, 2016.

[AD-3]   **ATBD** Algorithm Theoretical Basis Document for GOME-2 NO2 and H2O Level 3 Climate Products, SAF/O3M/DLR/ATBD/Clim, M. Grossi, et al., 2016.

[AD-4]   **ATBD** Algorithm Theoretical Basis Document HOAPS (2011) release 3.2 Ref Number: SAF/CM/DWD/ATBD/HOAPS. Andersson et al., 2011

[AD-5]   **PRD** O3M SAF Product Requirements Document, SAF/O3M/FMI/RQ/PRD/001/Rev. 1.7, J. Hovila, et. al., 2015

1.4 Structure of the report

The structure of this report is as follows.

Section 2 gives an overview of the GOME-2/MetOp-A and GOME-2/MetOp-B monthly gridded product together with a short description of the retrieval algorithm and the gridding approach used for the sampling of the L3 H_2O column. We also introduce the CM SAF HOAPS-4.0 data product used for the comparison and point out some of the differences with respect to the previously released HOAPS-3.2 Climatology. The validation strategy and outcomes of the comparison between AC SAF gridded monthly means and CM SAF TCWV are presented in Section 3. Finally, Section 4 contains detailed results concerning the seasonality and the spatial distribution of monthly mean biases between the GOME-2 and SSM/I observations.

2   Methods and reference data

2.1 GOME-2 total column water vapour product

The GOME-2 total column water vapour product is derived from measurements of the GOME-2 instruments aboard EUMETSAT polar-orbiting MetOp-A and B satellites. The GOME-2 instrument is a downward-looking spectrometer operating in the UV/VIS/near-IR wavelength region. It has a swath width of 1920 km and a ground pixel size of 40 x 80 km^2.

The algorithm used for the retrieval of the H_2O vertical column is based on the classical DOAS method (Wagner et al., 2011) and does not include explicit modeling of the atmospheric radiative transfer [AD-1, AD-2]. Slant columns of H_2O and O_2 are derived from the differential absorption structure in the spectral range between 614 and 683nm. After the DOAS fit, slant columns are corrected for saturation using model results from line-by-line calculations. The conversion from slant columns to vertical columns is performed applying the air mass factor of O_2, in conjunction with an AMF correction factor which accounts for different height profiles of H_2O and O_2. The algorithm deliberately uses a minimum of external input, in order to generate a data set, which is truly independent from global climate models and from other instruments. In the latest version of the retrieval algorithm (Grossi et al., 2015), a further enhancement in the quality of the H_2O total column is introduced by optimizing the cloud screening and developing an empirical correction in order to eliminate the instrument scan angle dependencies. The correction is based on the GOME-2A full time series and is computed separately over land and ocean surfaces, to take into account the diverse reflectivity properties of the surface.

In this report the AC SAF Level 3 Climate product is evaluated against the CM SAF HOAPS-4.0 product from SSM/I and SSMIS. The gridded GOME-2 data record is available as monthly means on a regular 0.5°x0.5° longitude/latitude grid and covers the years from 2007 to 2015 for GOME-2A and from 2013 to 2015 for GOME-2B. Besides the water vapour product, support data relative to the clouds and surface properties are included in the data set. An area weighted tessellation procedure is used to bin the product. Detailed information about the Level 2 retrieval method for GOME-2 and the aggregation and gridding procedure used to produce the Level 3 monthly products can be found in the AC SAF ATBD [AD-3].

Figure 2.1 shows the mean distribution of GOME-2A and GOME-2B monthly gridded TCWV data in April 2014. Mostly cloud-free conditions are considered. In contrast to other satellite data sets, the GOME-2 product has the advantage that it covers the entire Earth, including both ocean and continents, leading to a more consistent picture of the global distribution of the atmospheric humidity. Moreover, the retrieval is performed in the visible/near-infrared spectral range and it is very sensitive to water vapour in the lower troposphere, which contributes the major fraction of the total atmospheric column.

In the following we show a few plots with statistics of the product. These are presented as zonal averages (averaged over longitude grid cells), taking into account only the grid cells over ocean. The X-axis labelling denotes months from January 2007 to December 2014.

The average errors on the GOME-2A TCWV product are shown in Figure 2-2; these are shown as zonal averages of the monthly gridded data. For GOME-2B the errors are very similar.

Figure 2-3 shows the zonal averages of the internal RMS of the monthly gridded data. This may be taken as measure for the natural variability in-between the measurements. The variability is the largest for mid-latitudes in summer.

The zonal averaged cloud fraction from the gridded data is shown in Figure 2-4 for comparison. The cloud cover is largest in summer at higher latitudes. Note that this does not necessarily correspond to the geophysical cloud cover, because no TCVW has been calculated in the GOME level-2 product for "heavily clouded" pixels. Heavily clouded means here: (cloud fraction) x (cloud albedo) > 0.6 or O_2 column >80% obscured, see [ATBD]. Having said that, it would not be unexpected if regions with larger cloud fractions would turn out to have larger biases.

Ref:	SAF/AC/DLR/VR/L3_H2O				
Date:	06 November 2017				
Issue:	1	**Revision:**	1	**Page 13**	

EUMETSAT
AC SAF
ATMOSPHERIC COMPOSITION
MONITORING

The zonal sum of monthly observations is shown in Figure 2-5. This shows that the cloud screening still leaves a large number of monthly observations. At high latitudes we have (unsurprisingly) more observations in summer than in winter.
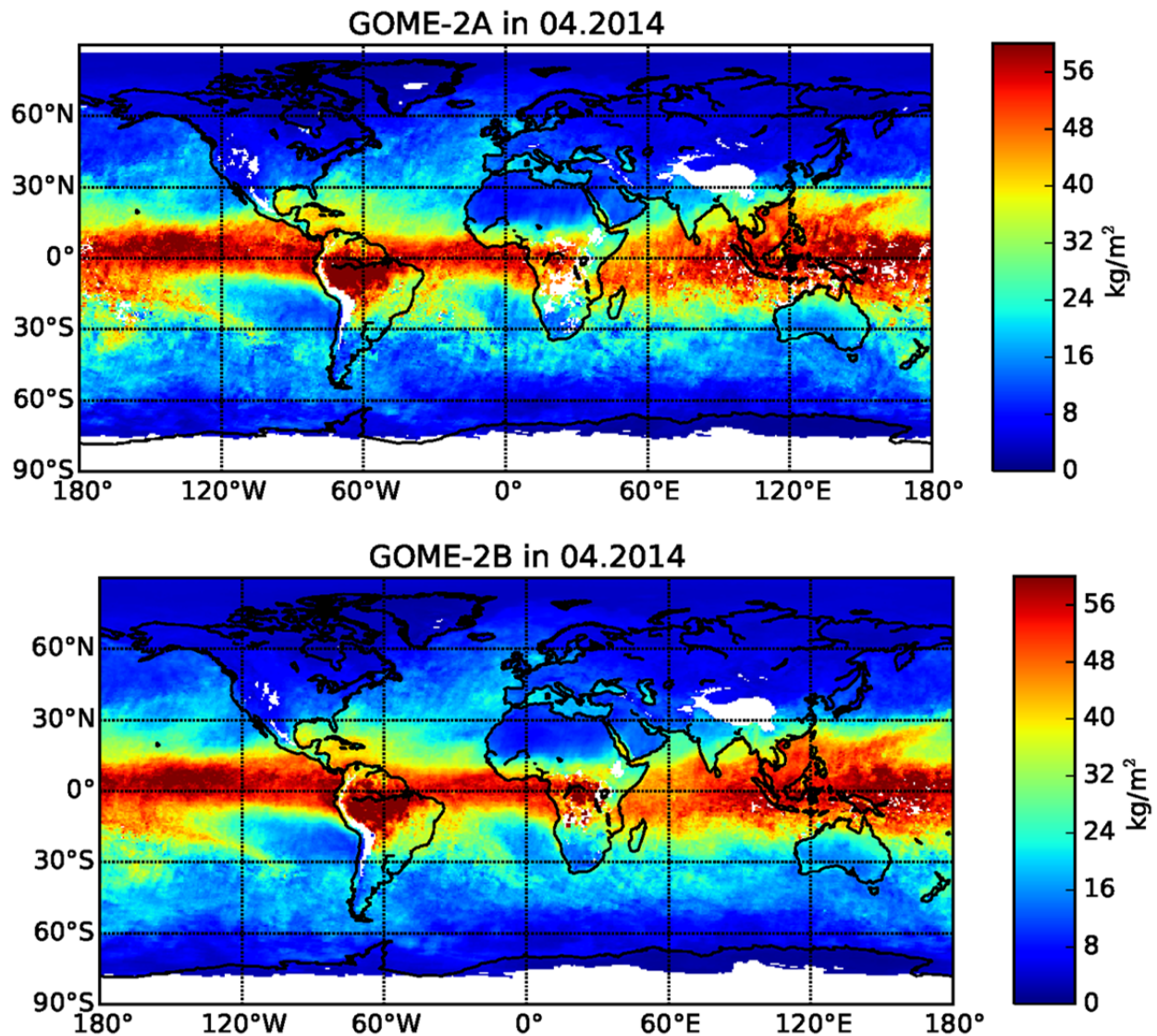

Figure 2-1: AC SAF Climate product: geographical distribution of the monthly mean H_2O vertical columns derived from GOME-2A (top panel) and GOME-2B (bottom panel) measurements in April 2014.
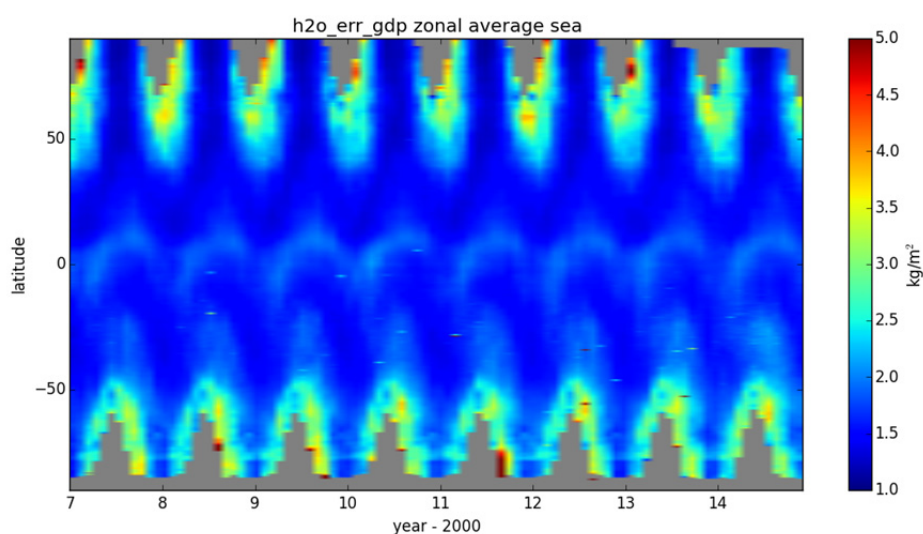
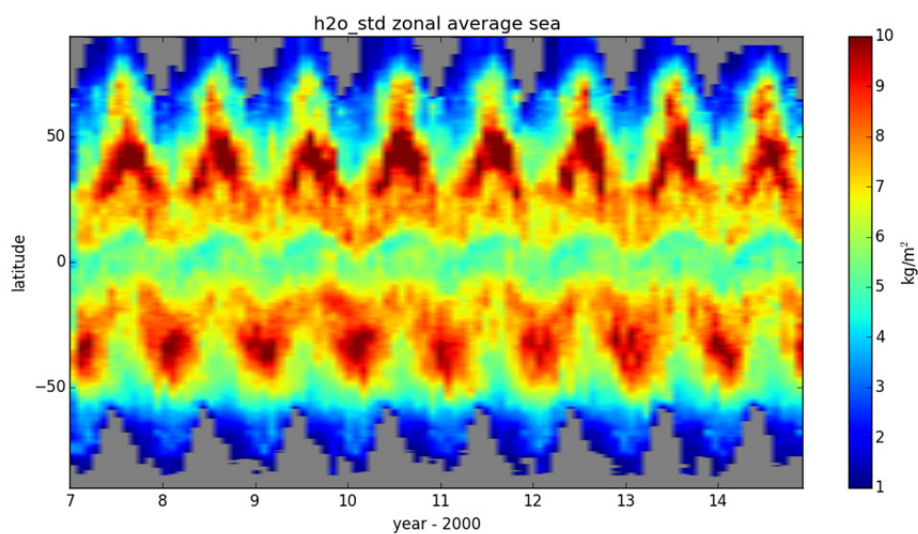Figure 2-2 Zonal average of the TCWV error on the monthly gridded GOME-2A product

Figure 2-3 Zonal average of the TCWV variability calculated for the monthly gridded GOME-2A product
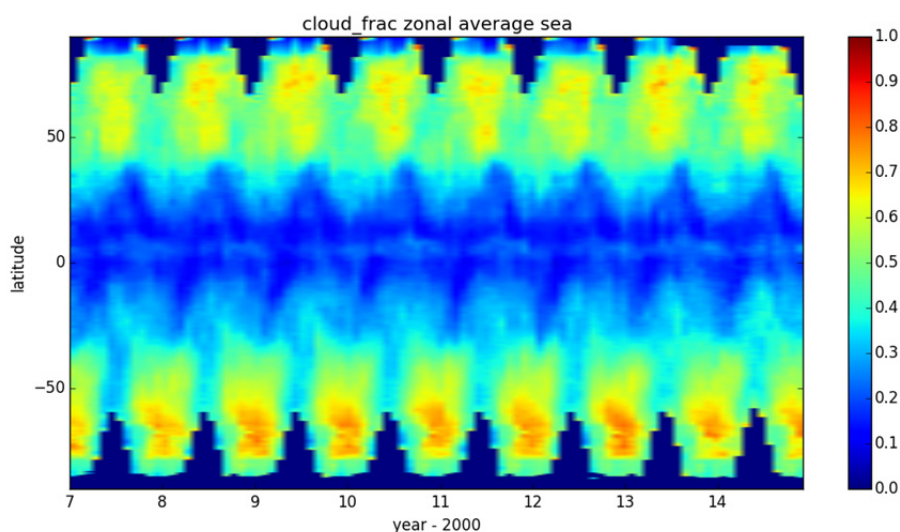
Figure 2-4 Zonal average of the cloud fraction for the monthly gridded GOME-2A TCWV; note that heavily clouded pixels are already omitted from the GOME level-2 TCWV product.
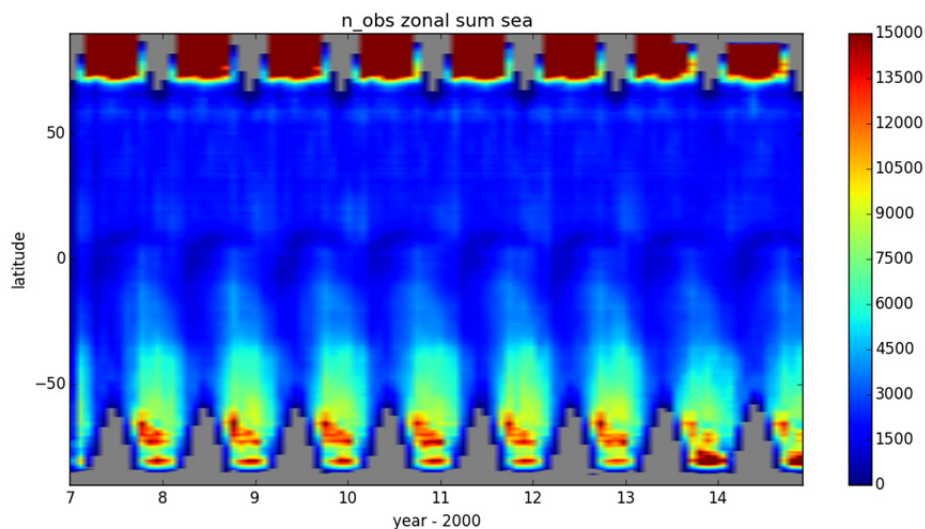

Figure 2-5 Zonal sum of number of monthly observations per latitude grid cell.

2.2 SSM/I HOAPS-4.0 total column water vapour product

In this report we compare the GOME-2 product with the CM SAF total column water vapour data record derived from SSM/I and SSMIS observations on-board the Defense Meteorological Satellite Program (DMSP) platforms, that is, the Hamburg Ocean Atmosphere Parameters and Fluxes from Satellite Data (HOAPS) (Jonas et al., 2009; Andersson et al., 2010; Fennig et al., 2012). The HOAPS products are widely used in the scientific community and have been positively evaluated in independent retrieval assessment (Schröder et al., 2013, Schröder et al., 2016).

The newly released HOAPS-4.0 climatology is available as monthly averages on a regular latitude/longitude grid with a spatial resolution of 0.5° x 0.5° from July 1987 to December 2014. It is based on data from SSM/I instruments on DMSP F-08, F-10, F11, F13, F14 and F15 platforms. In order to further extend the HOAPS product in time, data from the successor instrument SSMIS on DMSP F-16, F17 and F-18 were used from late 2005 onwards. All SSM/I and SSMIS instruments

have been carefully recalibrated, corrected and intercalibrated. Among others, the intercalibration is carried out as function of scene temperature and accounts for diurnal cycle effects (Fennig et al., 2017).

In HOAPS-4.0 a 1D-Var retrieval was implemented to retrieve, among others, TCWV with uncertainty estimates. The OISST (Optimum Interpolation Sea Surface Temperature) data set from NCEI was used as auxiliary input (see ATBD available online at http://www.camsaf.eu/docs). The HOAPS-4.0 data set has global coverage, within +/- 180° longitude and +/- 80° latitude. The product is only defined for ice-free oceanic surface, but it also includes TCWV for cloudy scenes, both day and night overpasses and spans a very large time range. It is available as monthly means and 6-hourly composites and it has been intensively validated (see validation report available online at http://www.cmsaf.eu/docs). As an example, the mean total column water vapour distribution from HOAPS for April 2014 is shown in Figure 2.6.

The validation report cites a bias w.r.t. the REMSS SSM/I algorithm of <0.4 kg/m^2 and an internal standard deviation between the algorithms of ~1 kg/m^2. Validation of an earlier HOAPS version (Bentamy et al.2003) showed a maximum bias w.r.t. in-situ data of ~2.5 kg/m^2 in summer. For the latest HOAPS version this bias may be expected to be smaller.
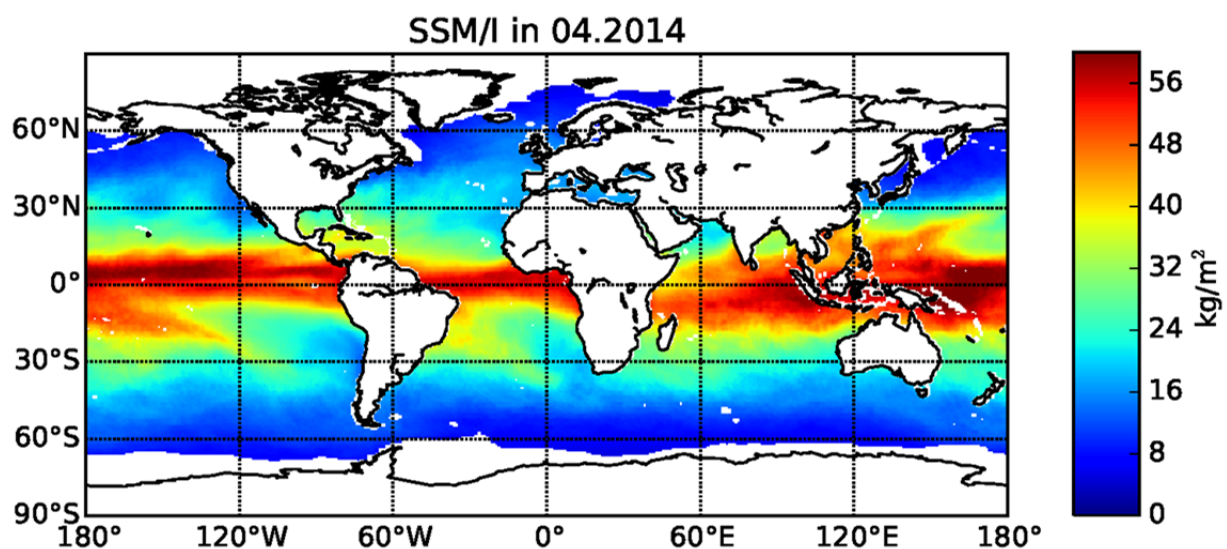

Figure 2-6: CM SAF HOAPS-4.0: geographical distribution of the monthly mean H$_2$O vertical columns derived from SSM/I and SSMIS measurements in April 2014.

Ref:	SAF/AC/DLR/VR/L3_H2O		
Date:	06 November 2017		
Issue:	1	**Revision:** 1	**Page 17**

EUMETSAT AC SAF
ATMOSPHERIC COMPOSITION MONITORING

3 GOME-2 AC SAF vs SSM/I CM SAF : Global comparison

3.1 Method

Monthly mean TCWV data from the GOME-2 instruments have been compared with the CM SAF SSM/I gridded product in the overlap period January 2007 to December 2014 (for GOME-2A) and January 2013 to December 2014 (for GOME-2B). Both water vapour data sets are gridded on a regular $0.5° \times 0.5°$ latitude/longitude grid. On average the number of collocations is of about 125000 grid cells in common (45-50% of the total grid size). Regions north of $+/-80°$ of latitude and land surfaces are not included in the SSM/I data set. In the GOME-2 product, observations are masked for cloudy conditions. Therefore, the comparisons are performed using only GOME-2 H_2O total columns which are not flagged as cloud-contaminated on the Level 2 data product. Due to the large number of observations (only 0.9% of all $0.5°$ latitude zones has less than 100 observations over ocean per month, the median lies near 2000 observations per latitude zone, see also Figure 2-5), biases will be calculated as simple averages, without a weighting with the number of observations. In the following Sections a quantitative analysis of the bias and RMS between the AC SAF and the CM SAF products is performed. A discussion of the global distribution of the differences as a function of latitude concludes this Chapter.

3.2 Mean bias time series

Figure 3.1 shows a time series of globally averaged absolute mean bias and mean RMS of the TCWV distribution between the AC SAF GOME-2 climate products and the CM SAF SSM/I data set for the time period between January 2007 and December 2014. The agreement is good for both comparisons: through the whole period the monthly bias (GOME-2 − SSM/I) ranges between -1.7 and +0.7 kg/m^2. A positive stability (0.147 +/-0.239 % per decade) is observed for the GOME-2A bias, which is consistent with the null hypothesis of 0% stability per decade (p-value= 0.54).

Further analysis of the GOME-2 and SSM/I intercomparison underlines a seasonal dependence in the results: the bias has systematically higher values in the northern hemisphere summer and lower values in the northern hemisphere winter months. The monthly averaged bias between GOME-2A and SSM/I ranges from a minimum of -1.702 kg/m^2 in January 2010 to a maximum of 0.417 kg/m^2 in July 2014 (blue line and points in Figure 3.1). Large seasonal variations (up 1.6 kg/m^2) in the distribution of the mean bias are also visible when plotting the bias between GOME-2B and SSM/I (green line and points in Figure 3.1). Interpreting these results, we should have in mind the limitations of GOME-2 retrieval. Although a specific advantage of the visible spectral region is that it is sensitive to the water vapour concentration close to the surface and that it has a comparable sensitivity over land and ocean, the accuracy of individual observations is, in general, reduced for cloudy sky conditions. Since the microwave instruments can measure the water vapour also below clouds, a seasonal cycle of the geographic distribution of the bias could be caused, among other reasons, by the seasonality of cloud properties, as well as the variability of the geographic distribution of major cloud structures as the Intertropical Convergence Zone (ITCZ).

When averaged over the full time series the mean bias is -0.7 kg/m^2 for the comparison with GOME-2A (blue line and points) and -0.3 kg/m^2 for the comparison with GOME-2B (green line and points), implying on average larger TCWV for the SSM/I data set. Since the GOME-2B total column data are typically larger than the GOME-2A data, also the bias is shifted towards higher (less negative) values in this case. These results demonstrate that the product fulfils the user requirements in terms of optimal accuracy (5%) stated in the Product Requirements Document [AD-5] as far as the systematically difference is concerned. On the other hand, the Root Mean Square Error (RMS) is larger, about 3.5 kg/m^2 on average. The RMS for the water vapour measurements is evaluated from the mean squared difference between the GOME-2 and the SSM/I data in each grid point and it has a relatively high value due to the high water vapour

	Ref:	SAF/AC/DLR/VR/L3_H2O			
	Date:	06 November 2017			
	Issue:	1	Revision:	1	Page 18

EUMETSAT
AC SAF
ATMOSPHERIC COMPOSITION
MONITORING

natural variations. The natural variability seems to be largest in summer, according to Figure 2-3. (the outlier for January 2007 corresponds to an unusual low number of observations, see also Figure 2-5). The overall results are summarized in Table 3.1 (these are the total averages of data plotted in Figures 3.1 and 3.2). The uncertainty margins provided for the bias and the RMSE statistics result from the spread of the bias and RMSE values in the time series.
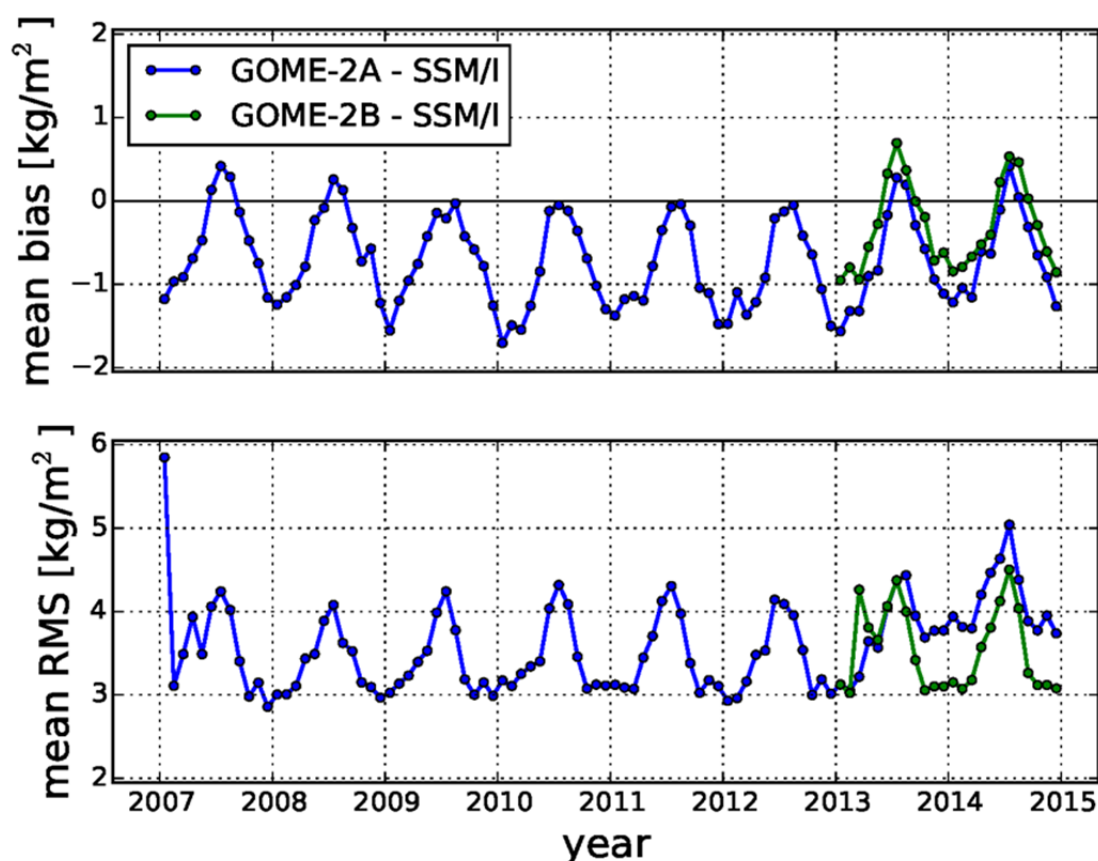

Figure 3-1: Global monthly mean bias (top panel) and mean RMS (bottom panel) of the AC SAF GOME-2A (blue points) and GOME-2B (green points) Level 3 data minus the CM SAF SSM/I climatology retrieved with the HOAPS-4.0 algorithm.

Data	Mean bias (kg/m^2)	RMSE (kg/m^2)	Median (kg/m^2)	25th PCTL (kg/m^2)	75th PCTL (kg/m^2)
GOME-2A – SSM/I (01.2007-12.2014)	-0.706 +/- 0.540	3.582 +/- 0.534	-0.607 +/- 0.396	-2.933 +/- 0.380	1.555 +/- 0.747
GOME-2B – SSM/I (01.2013-12.2014)	-0.309 +/- 0.516	3.542 +/- 0.493	-0.209 +/- 0.350	-2.538 +/- 0.304	1.965 +/- 0.730

Table 3.1: Bias and RMS statistics. All computations refer to the average difference between the AC SAF GOME-2 climate data and CM SAF monthly means from SSM/I and SSMIS observations retrieved using the HOAPS-4.0 algorithm. The time period analysed is January 2007 – December 2014 for the comparison GOME-2A – SSM/I, and January 2013 - December 2014 for the comparison GOME-2B - SSM/I.

A strong seasonal distribution of the bias can be also observed by looking at the median of the monthly bias between the GOME-2 products and the SSM/I observations (see Figure 3.2, magenta lines). The median bias is very close to the mean results (only slightly smaller), with larger positive values in the northern hemisphere summer months and lower negative values in the northern hemisphere winter months. In this case the amplitude of the winter-summer oscillations is 1.73 kg/m^2 (for GOME-2A) and 1.08 kg/m^2 (for GOME-2B) at most. The spread between the upper and lower quartile of the monthly data distribution (blue bars in the figure) is generally higher in the summer months (the only exception is January 2007, with an interquartile range of 6.8 kg/m^2).
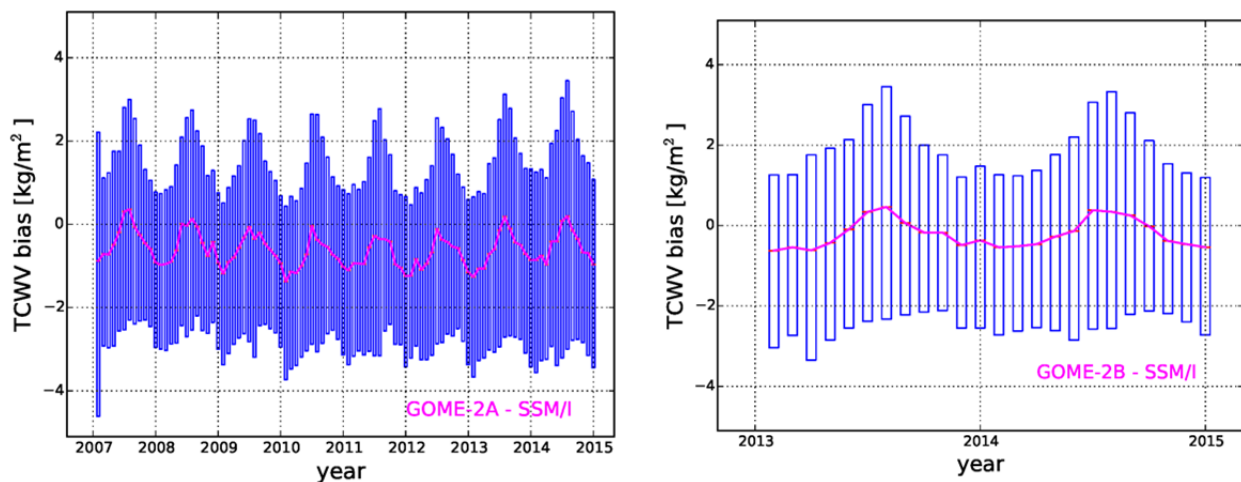

Figure 3-2: Global monthly median bias between the CM SAF SSM/I climatology retrieved with the HOAPS-4.0 algorithm and the GOME-2A (left panel) and GOME-2B (right panel) Level 3 data; blue bars indicate bias data between the 25% and 75% quantile.

3.3 Global distribution of the bias: Zonal average

In this Section we investigate the differences between the AC SAF GOME-2 Level 3 product and the CM SAF SSM/I data set as a function of latitude and season. For each month we compute the zonal average bias over all 0.5° latitude intervals.

The results are shown in Figure 3.3. The latitudinal dependence of the bias contribution for the comparison GOME-2A-SSM/I is illustrated in the left panel, while the right panel refers to the comparison GOME-2B-SSM/I. From these results we can infer that there is a good agreement between the products at all latitudes. Intense blue and red shading in the Figure indicates regions with higher negative and positive bias, respectively. As discussed in the previous Section, in general the GOME-2A data are drier than the SSM/I observations, but regions with positive absolute bias are clearly visible especially in the northern hemisphere summer months at higher latitudes (red stripes in the image). From the zonal plots in Section 2.1 we infer that the number of observations in [especially the southern] hemispheric summer is larger, which outside the [ant-]arctic implies that less pixels are rejected because of cloud cover in the GOME-2 data. At the same time, the average cloud fraction of the valid pixels is larger. Figure 3.3 then suggests that larger cloud fractions correlate with larger (less negative) bias. Results for GOME-2B are very similar but are limited to a shorter overlap time period. However, there is not necessarily a causal connection between cloud fraction and bias. Other relations such as increased surface albedo (possibly connected to wind speed), cloud-top height (in connection to the assumed H$_2$O vertical profile), or amount of maritime aerosol (for cloud-free pixels) might have an influence too.

   From a quantitative analysis, we found that the latitudinal averaged bias ranges between -6.7 kg/m^2 and +9.7 kg/m^2 (for GOME-A) and -5.37 kg/m^2 and +11.1 kg/m^2 (for GOME-B). The only exception is the bias higher than 12 kg/m^2 retrieved in November 2009 at latitude of about 70° north and associated to discrepancies in the Norwegian Sea. The number of grid points which contribute to the mean bias at this latitude is however very small. Apart from 2009, in the other years the largest bias values (both positive and negative) are predominantly located in the northern hemisphere summer months (June-August).

   Lower differences are present at lower latitude and in the southern hemisphere. Patterns in the inter-annual bias can be identified by looking at the distribution of white areas (bias close to 0) in the Figure: these are evident as band-like structure that can be seen through the time series. In particular, the characteristic structure and migration pattern of the ITCZ is visible through the year.
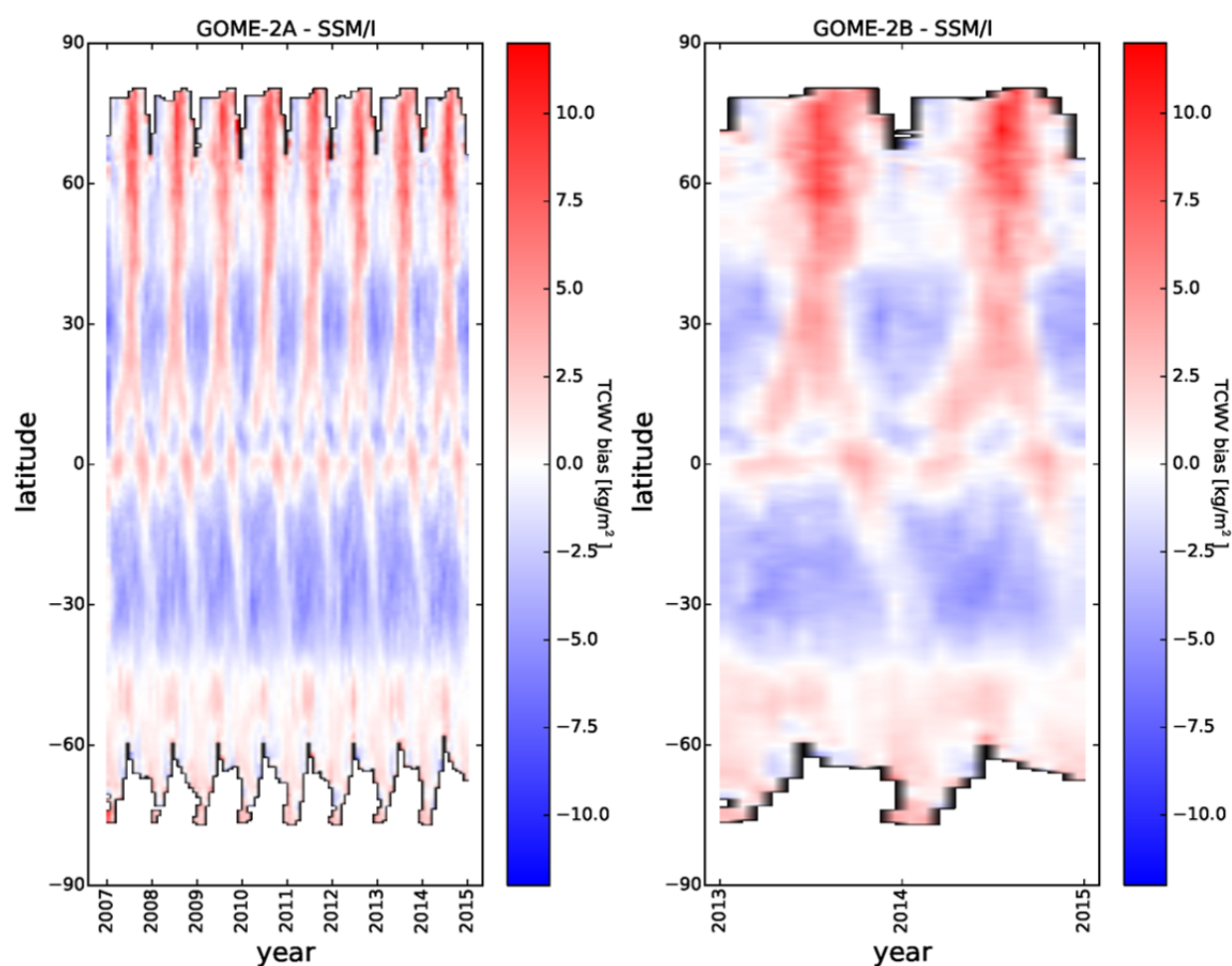

Figure 3-3: Contributions to the monthly bias between the GOME-2A and the SSM/I product (left panel) and the GOME-2B and the SSM/I product (right panel) as a function of the latitude bin.

Ref:	SAF/AC/DLR/VR/L3_H2O			
Date:	06 November 2017			
Issue:	1	Revision:	1	Page 21

EUMETSAT
AC SAF
ATMOSPHERIC COMPOSITION
MONITORING

4   GOME-2 AC SAF vs SSM/I CM SAF : Monthly comparison

4.1 Monthly bias and RMS: seasonal component

In this Section, the seasonal component of the bias between the AC SAF GOME-2 Level 3 data and the CM SAF SSM/I product is investigated (when not specified, "bias" refers to mean bias). In Figure 4.1 the mean and median bias and the associated standard deviations are aggregated by month over all years of our investigation: 2007 to 2014 for GOME-2A (left panel) and 2013 to 2014 for GOME-2B (right panel). Looking at the blue and green histograms we can notice a systematic variance in the retrieved values, with larger negative mean and median bias in our winter months and smaller positive bias in our summer months. On the other hand, the standard deviation associated to the bias measurements (red histograms) is in general larger in the summer months, since there is a larger spread in the data distribution.

Figure 4.2 shows the boxplot for the same bias data with the maximum whiskers length specified as 1.5 times the interquartile range. It refers to the comparison GOME-2A – SSM/I, while the results for GOME-2B are not shown due to the shorter time period available for the comparison. It can be seen that the variability of the bias around the median value inside each monthly bin is quite low, at most about 0.7 kg/m^2 in May (maximum interquartile range in April). The data sets are distributed quite symmetrically around the median value. Outliers are found in June 2007, February 2010, June 2011 and October 2011. In all cases the difference between the mean bias and the outliers is lower than 0.5 kg/m^2.

In the next Section we analysed two exemplary months (February and August 2014) in order to study the differences in the TCWV distribution on a local scale.
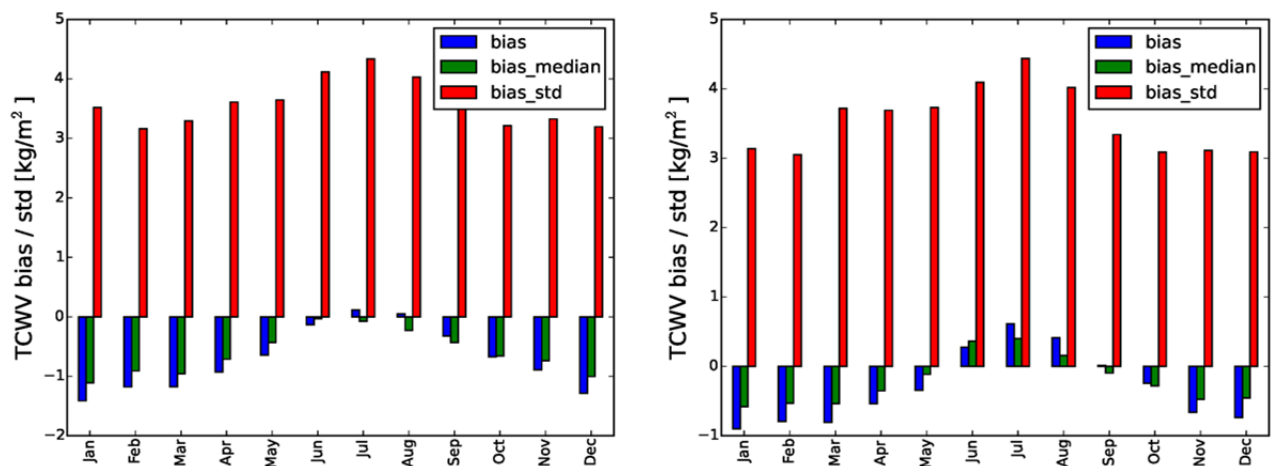

Figure 4-1: Mean bias (blue histograms), median bias (green histograms) and standard deviations (red histograms) derived from the comparison between the AC SAF GOME-2A (left panel) and GOME-2B (right panel) TCWV products and the CM SAF SSM/I cosmology and aggregated by months over the time period January 2007 to December 2014 (for GOME-2A) and January 2013 to December 2014 (for GOME-2B).

Ref:	SAF/AC/DLR/VR/L3_H2O			
Date:	06 November 2017			
Issue:	1	Revision:	1	Page 22

EUMETSAT AC SAF
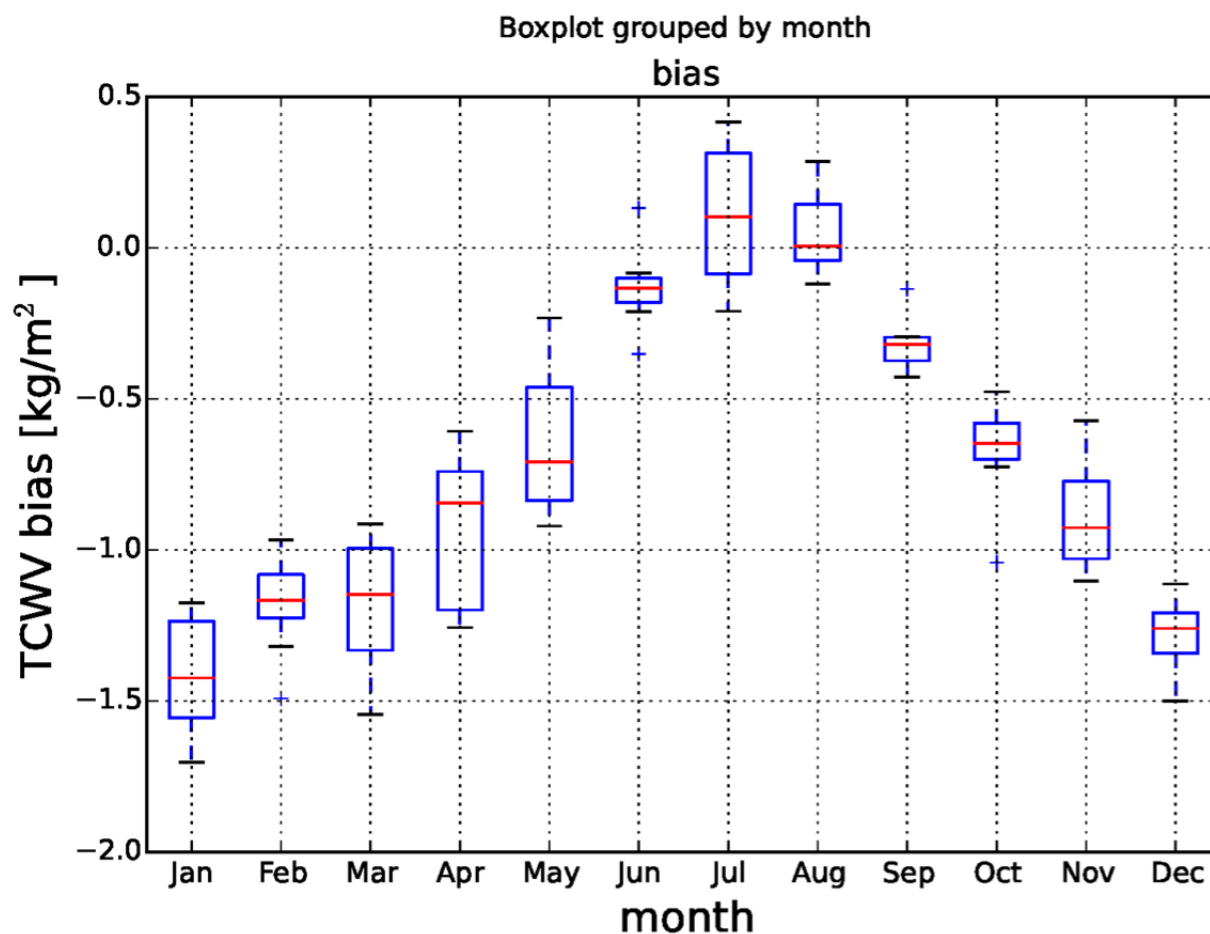ATMOSPHERIC COMPOSITION MONITORING

Figure 4-2: Box plot of the bias between the CM SAF SSM/I TCWV and the GOME-2A Level 3 data aggregated by month over the time period January 2007 to December 2014: blue boxes indicate spreads in average monthly bias between the 25% and 75% quantile, red bars indicate the median, whisker length is 1.5 times interquantile range, blue plusses are outliers.

4.2 Geographical distribution of the bias for exemplary months

Figure 4.3 and Figure 4.4 show the global monthly bias between GOME-2 and SSMIS observations in February and August 2014. The land regions are masked in the comparison, because the SSMIS data set is available only over ocean scenes, but microwave sensors can retrieve TCWV also in the presence of clouds and for night time satellite overpasses. Since we evaluate the bias between the two TCWV products from monthly mean data, and the underlying observations are masked for cloud-contaminated area in the GOME-2 data but not in the SSM/I data set, a larger and negative bias is expected to be found in the comparison. A daily co-locations selection, on the other hand, would minimize the effects of temporal change and cloud-contamination as shown in previous GDP 4.8 validation reports (Grossi et al., 2015).

In February 2014, the bias between GOME-2 and SSM/I is large and negative (–1.04 kg/m^2 for GOME-2A and –0.79 kg/m^2 for GOME-2B). However, by looking at the top panel of Figure 6.4, we observe also quite small positive discrepancies, especially for ocean regions in the southern hemisphere. As expected, since the GOME-2B data are wetter than the GOME-2A data, the mean bias is more positive in this case (about 0.25 kg/m^2 lower), but reaches values up to -10 kg/m^2 in some areas, namely the South Pacific Ocean near the coasts of Chile and the North Pacific Ocean east of Japan. The same patterns in the bias distribution are clearly recognizable in the GOME-2A and GOME-2B comparisons. Consistently with the bias results, the RMS is quite high: 3.82 kg/m^2 for GOME-2A and 3.07 kg/m^2 for GOME-2B.

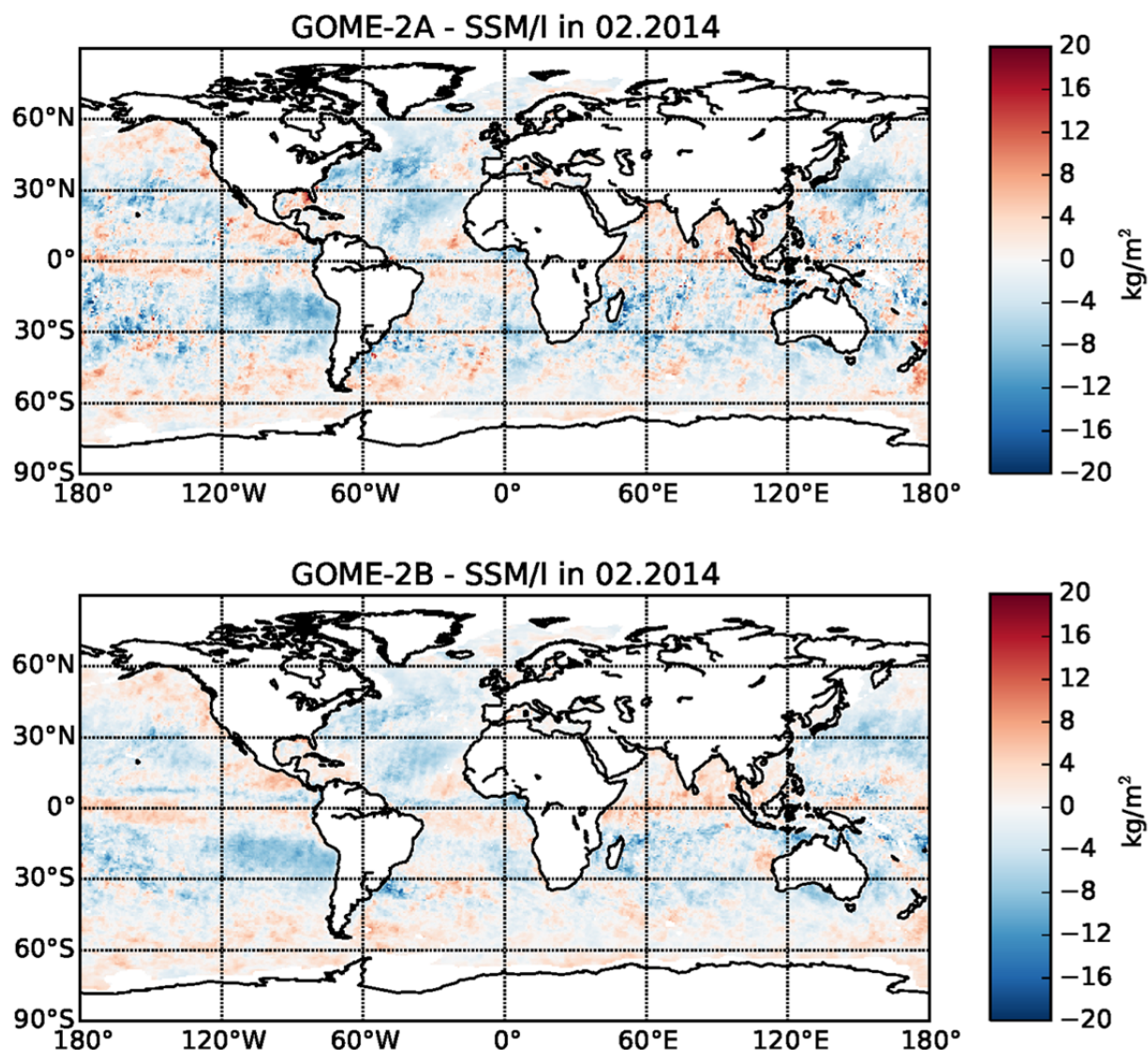|	Ref:	SAF/AC/DLR/VR/L3_H2O		
	Date:	06 November 2017		
	Issue: 1	Revision: 1		Page 23

EUMETSAT
AC SAF
ATMOSPHERIC COMPOSITION MONITORING

Figure 4-3: Geographical distribution of the differences observed comparing the AC SAF GOME-2A (top panel) and GOME-2B (bottom panel) Level 3 TCWV data with the CM SAF SSM/I HOAPS-4.0 climatology in February 2014.

We retrieve an even larger spread in the distribution of the bias values when comparing the products in the northern hemisphere summer months. In August 2014 the globally averaged differences between the GOME-2 and SSM/I measurements is 0.04 kg/m^2 and 0.46 kg/m^2 for GOME-2A and GOME-2B, respectively. Looking at Figure 4.4, a large positive bias is clearly visible in regions at high latitude, in particular the northern areas of the Atlantic and Pacific Ocean. At northern latitudes (45 - 75 degree north) the bias typically ranges between 1.3 and 7.1 kg/m^2, but more than 10% of the map bins have bias values larger than 10 kg/m^2. These areas are the dominating causes for the pronounced seasonal component in GOME-2 -SSM/I comparison. These differences were already observed in the comparison between the GOME-2 Level 2 product and ECMWF ERA-Interim simulated data set, the SSMIS F16 satellite data from REMSS and the GlobVapour SSM/I+MERIS combined product (Grossi et al., 2015). Higher bias was found to be associated to GOME-2 measurements with higher cloud fraction values (> 0.5). In Figure 4.5 we report the global distribution of the cloud fraction for GOME-2A-SSM/I co-locations in August 2014. Cloud and surface properties are also included in the AC SAF product. Residual cloud contamination is visible especially in the Bering Sea and in the northern coast of the European

continent. Intermediate values of cloud fraction are found at high latitudes and in the Southern Ocean.
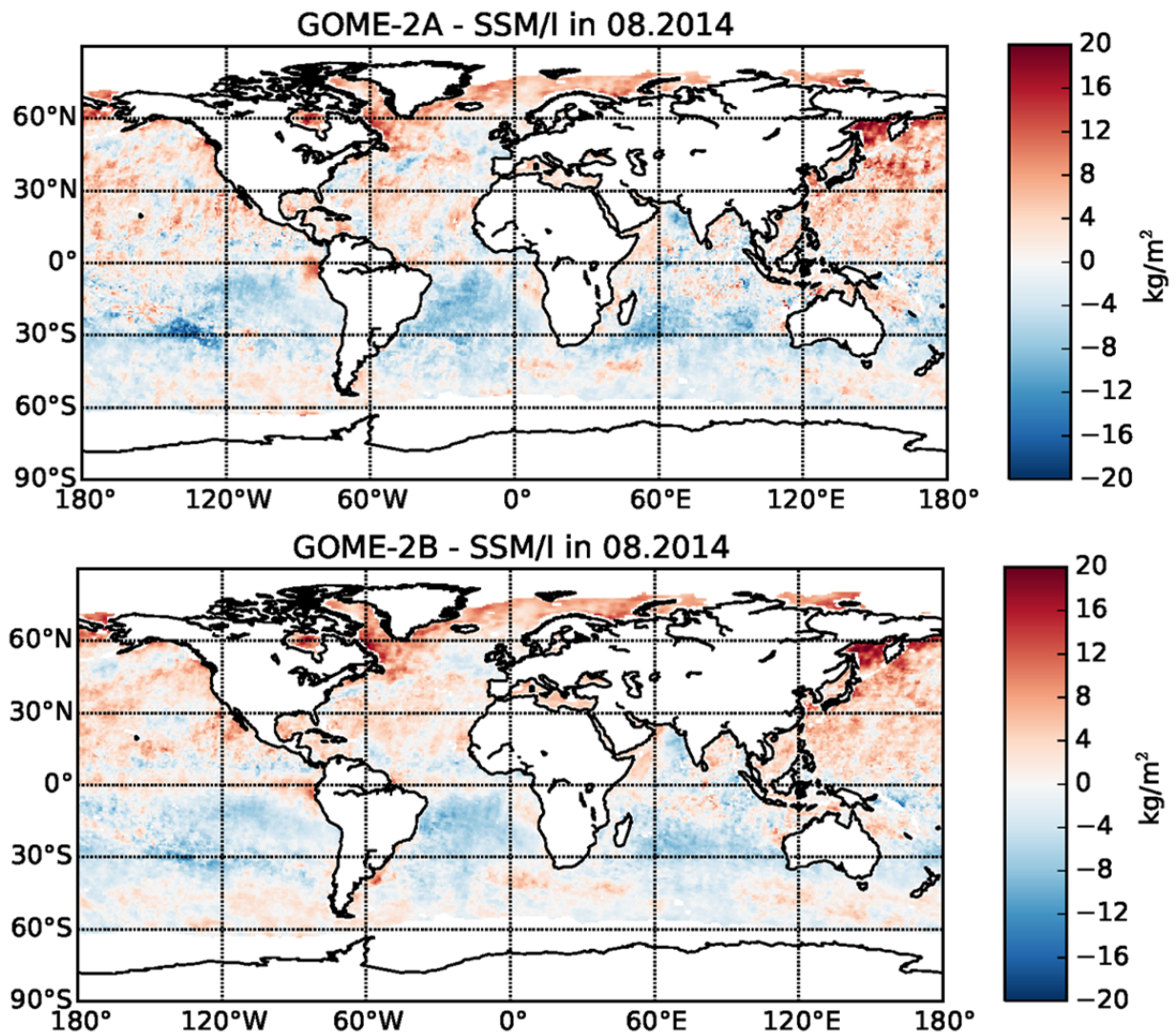

Figure 4-4: Geographical distribution of the differences observed comparing the AC SAF GOME-2A (top panel) and GOME-2B (bottom panel) Level 3 TCWV data with the CM SAF SSM/I HOAPS-4.0 climatology in August 2014.

Figures 4.6 and 4.7 show scatter plots of TCWV from the AC SAF GOME-2 versus the CM SAF SSM/I product for February and August 2014. The results for GOME-2A and GOME-2B data are comparable. In August 2014 a larger scatter is visible for intermediate TCWV values (around 25 kg/m^2). For each scatter plot, also the histogram representing the distribution of bias values for all comparisons is shown. It can be noticed that while in February 2014 the tail of the distribution is more extended toward negative bias values, both histograms have a positive skewness in August 2014.
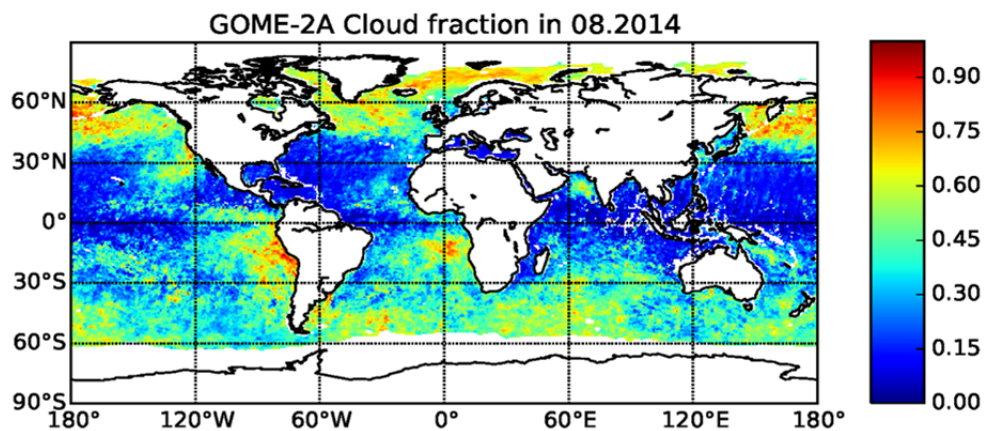
Figure 4.5: Geographical distribution of the residual cloud fraction in the co-located grid points used for the comparison between GOME-2A and SSM/I. The cloud fraction is retrieved with the OCRA algorithm.
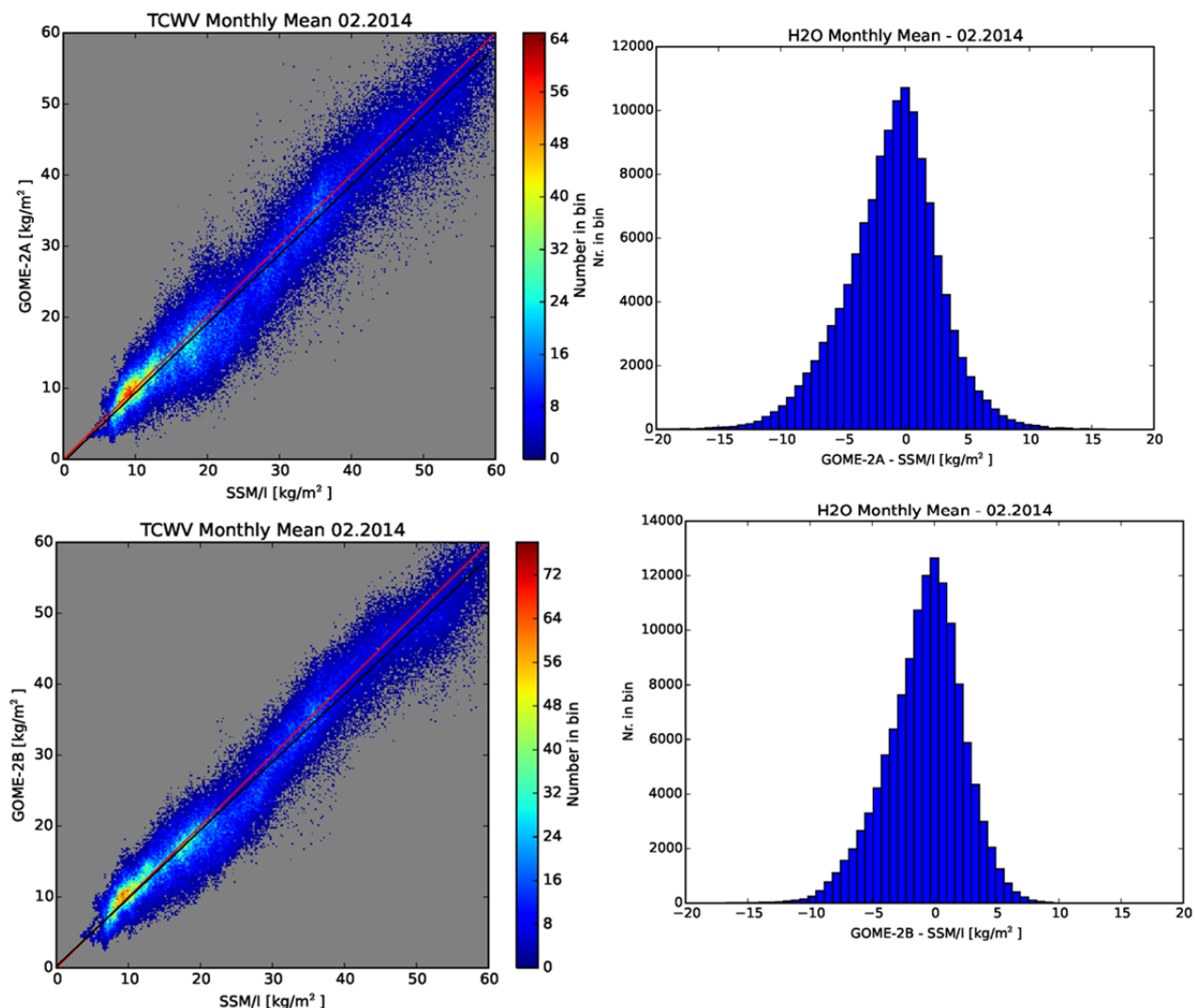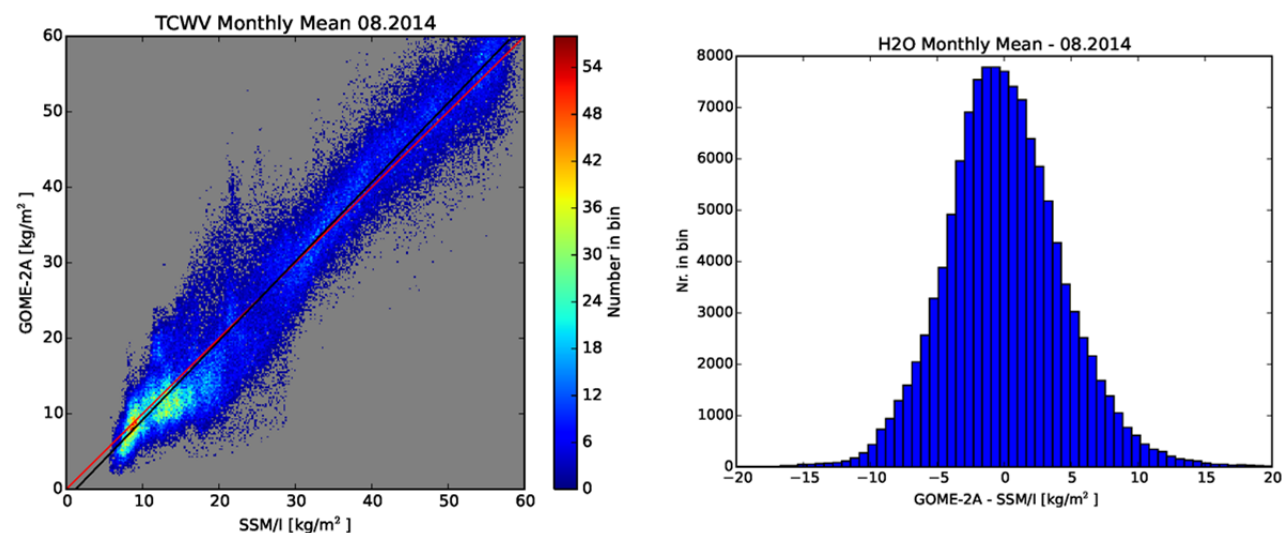
Figure 4-6: Top panel: scatter plot of the CM SAF SSM/I HOAPS-4.0 TCWV product against the AC SAF GOME-2A observations in February 2014 (left panel) and histogram of the difference for the points in the scatter plot. Bottom panel: same for GOME-2B.
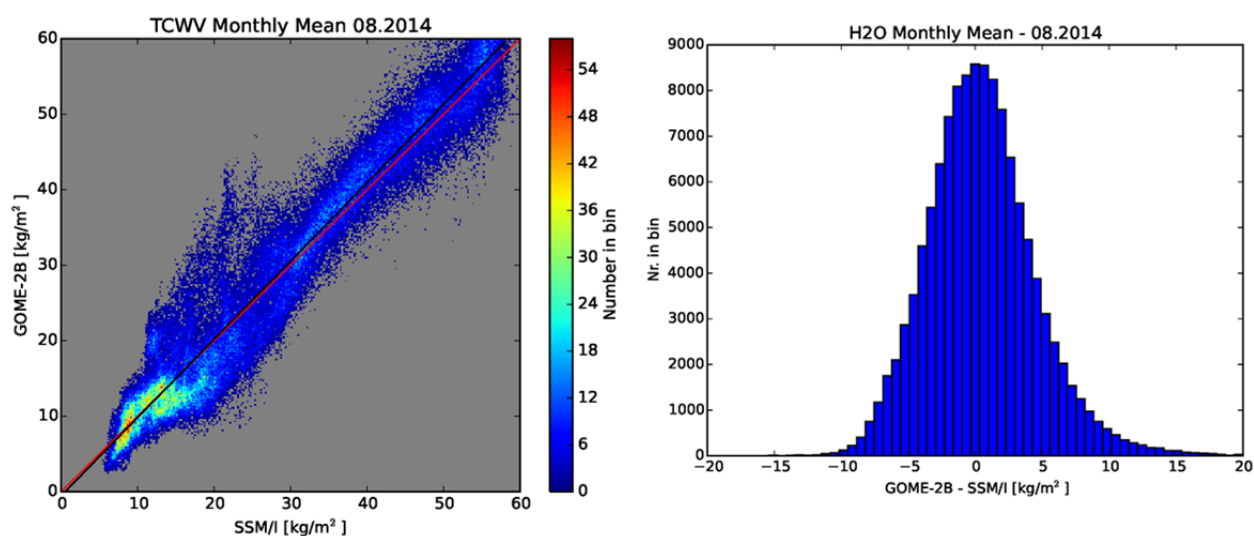
Figure 4-7: Top panel: scatter plot of the CM SAF SSM/I HOAPS-4.0 TCWV product against the AC SAF GOME-2A observations in August 2014 (left panel) and histogram of the difference for the points in the scatter plot. Bottom panel: same for GOME-2B.

Ref:	SAF/AC/DLR/VR/L3_H2O			
Date:	06 November 2017			
Issue:	1	Revision:	1	Page 28

EUMETSAT AC SAF
ATMOSPHERIC COMPOSITION MONITORING

5   Reference documents

Andersson, A., K. Fennig, C. Klepp, S. Bakan, H. Graßl, and J. Schulz, 2010: *The Hamburg Ocean Atmosphere Parameters and Fluxes from Satellite Data - HOAPS-3*, Earth Syst. Sci. Data, 2, 215-234, doi:10.5194/essd-2-215-2010

Bentamy, A., Katsaros, K. B., Mestas-Nunez, A. M., Drennan, W.M., Forde, B. E., and Roquet, H.: *Satellite estimates of wind speed and latent heat flux over the global oceans*, J. Climate, 16, 637–655, 2003

Fennig, Karsten; Andersson, Axel; Bakan, Stephan; Klepp, Christian-Phillip; Schröder, Marc. (2012): *Hamburg Ocean Atmosphere Parameters and Fluxes from Satellite Data - HOAPS 3.2 – Monthly Means / 6-Hourly Composites. Satellite Application Facility on Climate Monitoring.* DOI:10.5676/EUM_SAF_CM/HOAPS/V001. http://dx.doi.org/10.5676/EUM_SAF_CM/HOAPS/V001

Fennig, Karsten, Schröder, Marc. (2017): *Fundamental Climate Data Record of Microwave Imager Radiances, Edition 3. Satellite Application Facility on Climate Monitoring.* DOI:10.5676/EUM_SAF_CM/FCDR_MWI/V003. http://dx.doi.org/10.5676/EUM_SAF_CM/FCDR_MWI/V003

Grossi, M., Valks, P., Loyola, D., Aberle, B., Slijkhuis, S., Wagner, T., Beirle, S., and Lang, R.: *Total column water vapour measurements from GOME-2 MetOp-A and MetOp-B*, Atmos. Meas. Tech., 8, 1111-1133, doi:10.5194/amt-8-1111-2015, 2015

Grossi, M., Kalakoski, N., Valks, P.: *O3M SAF Validation Report, Offline Total Water Vapour*, SAF/O3M/DLR/ORR/H2O, 2015

Hollinger, J. P., Peirce, J. L., and Poe, G. A.: *SSM/I Instrument Evaluation*, IEEE Trans. Geosci. Remote Sens., 28, 781–790, 1990

Jonas, Markus; Schröder, Marc; Schulz, Jörg; Andersson, Axel; Bakan, Stephan; Fennig, Karsten; Grassl, Hartmut; Klepp, Christian-Phillip. (2009): *Vertically Integrated Water Vapour from SSM/I - Daily / Monthly Means. Satellite Application Facility on Climate Monitoring.* DOI:10.5676/EUM_SAF_CM/HTW_SSMI/V001. http://dx.doi.org/10.5676/EUM_SAF_CM/HTW_SSMI/V001

Schlüssel, P. and Emery, W. J.: *Atmospheric Water-vapor Over Oceans from SSM/I Measurements*, Int. J. Remote Sens., 11, 753–766, 1990

Schröder, M., Jonas, M., Lindau, R., Schulz, J., and Fennig, K. (2013): *The CM SAF SSM/I-based total column water vapour climate data record: methods and evaluation against re-analyses and satellite*. Atmos. Meas. Tech., 6, 765–775, doi:10.5194/amt-6-765-2013

Schröder, M., M. Lockhoff, J. Forsythe, H. Cronk, T. H. Vonder Haar, R. Bennartz: T*he GEWEX water vapor assessment (G-VAP) – results from the trend and homogeneity analysis*. J. Applied Meteor. Clim., 1633-1649, 55 (7), doi: /10.1175/JAMC-D-15-0304.1, 2016

Annex 3.2: Validation of GOME-2 Level 3 TCWV data record with ground based observations (CM SAF report)

The EUMETSAT
Network of
Satellite
Application
Facilities

CM SAF
Climate Monitoring

Product Validation Report
GOME-2 vs. NCAR GNSS
GOME-2 vs. GRUAN

Reference Number:	**SAF/CM/DWD/FA/GOME-2**
Issue/Revision Index:	**1.0**
Date:	**06.09.2016**

Report Change Record

Report Version	Date	Changes	Originator
Draft	2016.08.18	Original version	H. Höschen, M. Schröder
1.0	2016.09.06	After consolidation with DLR	H. Höschen, M. Schröder
1.1	2017.11.10	Several updates after DRR	P. Valks

1. Introduction

1.1 Purpose

This report presents the results of the comparison of monthly Total Column Water Vapor (TCWV) measurements from the ultraviolet spectrometer Global Ozone Monitoring Experiment-2 (GOME-2) on METOP-A and METOP-B and the Global Navigation Satellite System GNSS as well as the GCOS Reference Upper Air Network (GRUAN) radiosonde data records as reference. The investigation considers bias, RMS and stability as well as zonal and seasonal dependencies using data from 2007-2015.

This comparison is carried out within a Federated Activity between AC SAF and CM SAF during CDOP2. The major objective of the FA was to cooperate on the evaluation of GOME-2 water vapour products.

1.2 Definitions, acronyms and abbreviations

AC SAF   EUMETSAT Satellite Application Facility on Atmospheric Composition Monitoring

CM SAF   EUMETSAT Satellite Application Facility on Climate Monitoring

EUMETSAT   European Organisation for the Exploitation of Meteorological Satellites

GCOS   Global Climate Observing System

GOME-2   Global Ozon Monitoring Experiment-2

GNSS   Global Navigation Satellite System

GRUAN   GCOS Reference Upper-Air Network

METOP   Meteorological Operational Satellite

RMS   Root Mean Square Error

TCWV   Total Column Water Vapor

1.3 Applicable documents

[AD-1]   Wang, J., L. Zhang, A. Dai, T. Van Hove, and J. Van Baelen (2007), A near-global, 2-hourly data set of atmospheric precipitable water from ground-based GPS measurements, J. Geophys. Res., 112, D11107, doi:10.1029/2006JD007529.

[AD-2]   http://www.dwd.de/EN/research/international_programme/gruan/home.html

[AD-3]   http://www.dwd.de/EN/research/international_programme/gruan/sites.html

[AD-4]   http://docs.scipy.org/doc/scipy/reference/generated/scipy.stats.linregress.html

1.4 Reference documents

[RD-1]   Hyland, R.W., A Wexler (1983), "Formulations for the thermodynamic of the saturated Phases of H_2O from 173.15K to 473.15K, ASHRAE Trans, 89(2A), 500-519.

[RD-2]   E. Obligis, L. Eymard, N. Tran, S. Labroue, and P. Femenias, 2006: First Three Years of the Microwave Radiometer aboard Envisat: In-Flight Calibration, Processing, and Validation of the Geophysical Products. J. Atmos. Oceanic Technol., 23, 802–

814.doi: http://dx.doi.org/10.1175/JTECH1878.1

[RD-3] Ross, R.J., W.P. Elliot (1996), Tropospheric Water Vapor Climatology and Trends over North America: 1973-93, J. Climate, 9, 3561-3574, doi: 10.1175/1520-0442(1996)009<3561:TWVCAT>2.0.CO;2

[RD-4] Courcoux, N. and Schröder, M.: The CM SAF ATOVS data record: overview of methodology and evaluation of total column water and profiles of tropospheric humidity, Earth Syst. Sci. Data, 7, 397-414, doi:10.5194/essd-7-397-2015, 2015.

[RD-5] Sommer, Michael; Dirksen, Ruud; Immler, Franz. (2012): RS92 GRUAN Data Product Version 2 (RS92-GDP.2). GRUAN Lead Centre. DOI:10.5676/GRUAN/RS92-GDP.2

[RD-6] ATBD Algorithm Theoretical Basis Document for GOME-2 NO2 and H2O Level 3 Climate Products, SAF/O3M/DLR/ATBD/Clim, M. Grossi et al., 2016.

1.5 Structure of the report

An overview of the GOME-2, GNSS and GRUAN datasets and the methodology is given in section 2. Section 3 and 4 then present the comparison of the GOME-2 data to both reference datasets. In section 5 conclusions are given.

2. Methods and reference data

2.1 GOME-2

The GOME-2 instrument is a downward-looking spectrometer operating in the UV/VIS/near-IR wavelength region. GOME-2 has a swath width of 1920 km and a ground pixel size of 40 x 80 km^2. For the retrieval of water vapour, a spectral window around the water vapour absorption lines near 630 nm is used. The retrieval can be employed both over ocean and over land surfaces. Detailed information about the Level 2 retrieval method for GOME-2 and the aggregation/gridding procedure to product gridded monthly products can be found in the AC SAF ATBD [RD-6]. The gridded GOME-2 TCWV data record is available as monthly means on a regular 0.5°x0.5° longitude/latitude grid and covers the years 2007-2015.

2.2 GNSS

The atmospheric delay of the signal sent by a satellite and received by a ground station is depending on pressure, temperature and total amount of water vapor, where the latter can be calculated by knowledge of pressure and temperature. Those were gained from synoptic observations as well as from the reanalysis of NCEP/NCAR. The GNSS data base version 721.1 includes data from 1995 to 2014. In total, 997 stations are specified. More information and calculations of the GNSS data base can be found in [AD-1]. A map of the global distribution of collocated stations is shown in section 3.

2.3 GRUAN

The radiosounding network GRUAN (GCOS Reference Upper Air Network) currently consists of 14 stations and includes radiosounding profiles from 0, 6, 12 and 18 UTC for the years 2005 to 2014, with temporal coverage and resolution being a function of station. Figure 2-1 displays the locations of the GRUAN stations and their current status (note that the GRUAN network is expanding and new stations will be established in the coming years), however, only Barrow, Boulder, Cabauw, Lamont, Lauder, Lindenberg, Manus, Nauru, Ny-Ålesund, Payenne, Potenza, Sodankylä and Tateno were collocated. The GRUAN data in version RS92_GDP_v2 [RD-5] was downloaded from ftp://ftp.ncdc.noaa.gov/pub/data/gruan/processing/level2/, and include, among others, profiles of relative humidity, temperature and pressure. More information about the GRUAN data record can be found in [AD-2].

Doc:	SAF/AC/DLR/VR/L3_H2O				
Date:	06 November 2017				
Issue:	1	Revision:	1		Page 34

EUMETSAT
AC SAF
ATMOSPHERIC COMPOSITION MONITORING

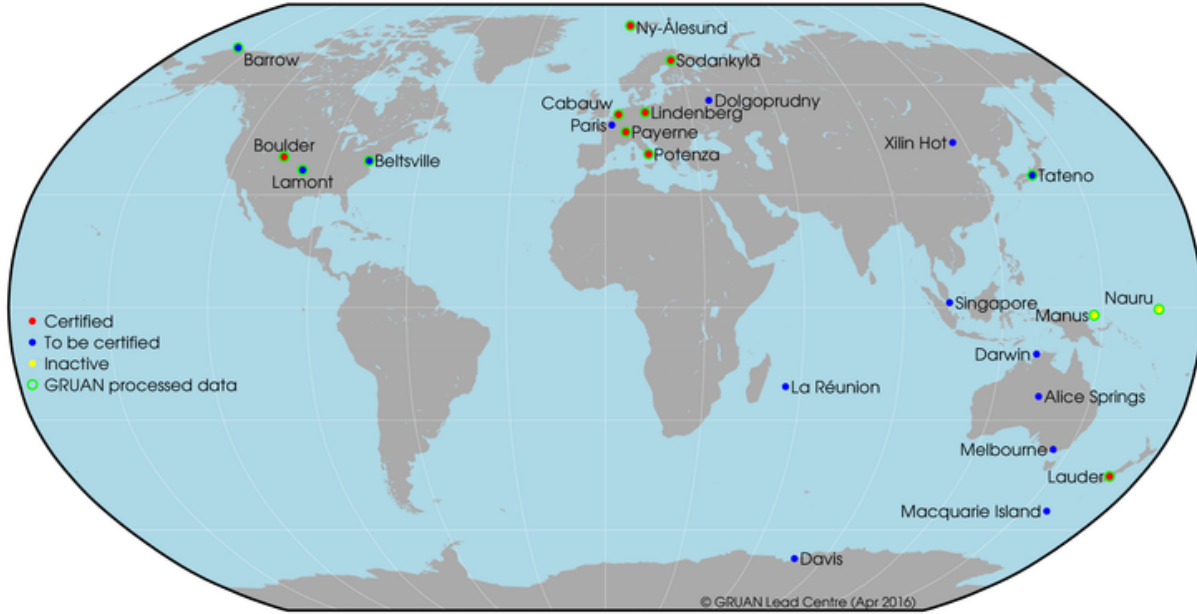GCOS Reference Upper-Air Network

Figure 2-1: Locations and status of the GRUAN stations [AD-3].

2.4 Methodology

We compare monthly mean TCWV data of GOME-2 with monthly mean TCWV data of NCAR GNSS and GRUAN.

The GRUAN data record is based on relative humidity profiles, a conversion to TCWV is therefore necessary and done using the saturation water vapor pressure e_s [Pa] as calculated in [RD-1]

$$Log(e_s) = \frac{5800.2206}{T} + 1.3914993 - 0.048640239T + 0.000041764768T^2$$
$$- 0.14452093 * 10^{-7}T^3 + 6.5459673 * Log(T) , \qquad (1)$$

with temperature T in [K] to calculate the specific humidity sh [kg/kg]:

$$sh = \frac{0.622 * e_s * rh}{p - 0.378 * e_s * rh} , \qquad (2)$$

where rh is the relative humidity in [%], p the pressure in [hPa].

TCWV can then be calculated by integrating the profile from surface to top of the atmosphere:

$$TCWV = \frac{1}{9.81} \int_{p\_surface}^{p\_top} sh \, dp \tag{3}$$

Note that the dependence of *sh* on altitude dependent temperature is accounted for by computing *sh* using $rh(p)$ and $e_s(T(p))$, see Eq. 1 and 2.

Since the data of GOME-2 was given as monthly means, GNSS as well as GRUAN data were averaged on a monthly basis, using the arithmetic mean of all valid values of a month for each station:

$$TCWV_{monthly\_mean} = \frac{\sum TCWV_i}{n}, \tag{4}$$

with *n* being the number of valid observations.

The collocation criterion is 100 km maximum distance, as often seen in literature, e.g. [RD-2]. These collocations were then again reduced by checking if their longitudes as well as their latitudes differ by only $0.5°$ to be conform with the $0.5°$-grid of GOME-2. Only the nearest neighbor is used if several collocations were found at the same GNSS/GRUAN station. Only stations providing at least 10 collocations were taken into account.
GNSS stations with altitudes above 500 meters were declined for two reasons: first, if a station is located on a small island the difference in average elevation between the station and the satellite in combination with a strong decrease in water vapour content with height will cause a large difference. Second, for stations over land the surface elevation might vary strongly over the Level 3 grid box which will lead to systematic deviations when comparing the satellite data to more localised ground-based data.

The stability analysis is based on linear least-square regressions, see [AD-4]. Bias as well as a bias-corrected RMS are provided.

3. GOME-2 vs GNSS

The number of collocations between GNSS and GOME-2A and between GNSS and GOME-2B is displayed in figure 3-1. Even though the northern hemisphere includes most of the stations, the global coverage is reasonable. The lower number of collocations for GOME-2B is caused by the late launch of METOP-B.
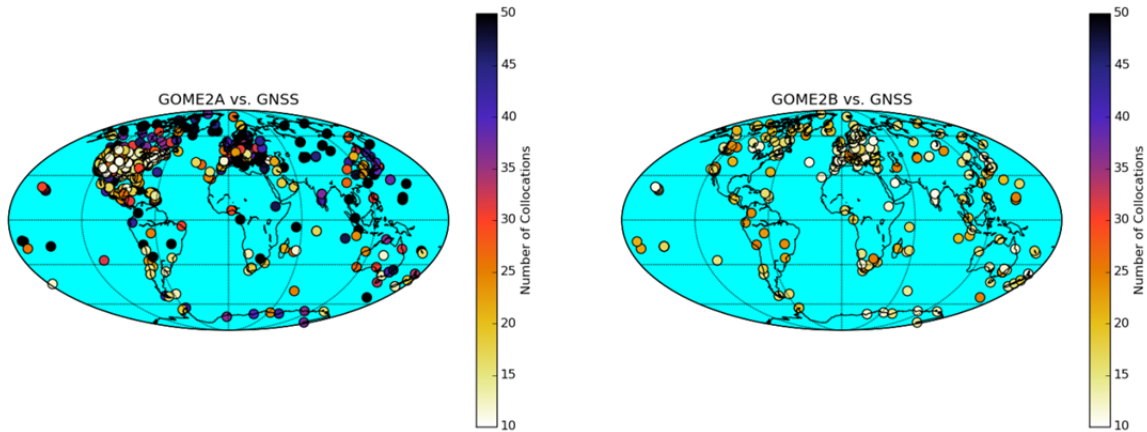

Figure 3-1: Global distribution of the number of collocations of each station for GOME-2A (left) and GOME-2B (right).

3.1 Stability

The time series of the monthly mean bias, averaged over all stations with more than 10 collocations is displayed in figure 3-2. A positive stability (0.14 ± 1.86 %/decade) for GOME-2A is observed. The p-value is 0.94. Thus, the null hypothesis, that the stability is 0%/decade needs is not rejected, leading to the interpretation that the stability is not significantly different from 0%/decade. Note that the analysis of stability is hardly possible due to the short temporal coverage. We have not included the stability estimation for GOME-2B due to the even shorter temporal coverage.
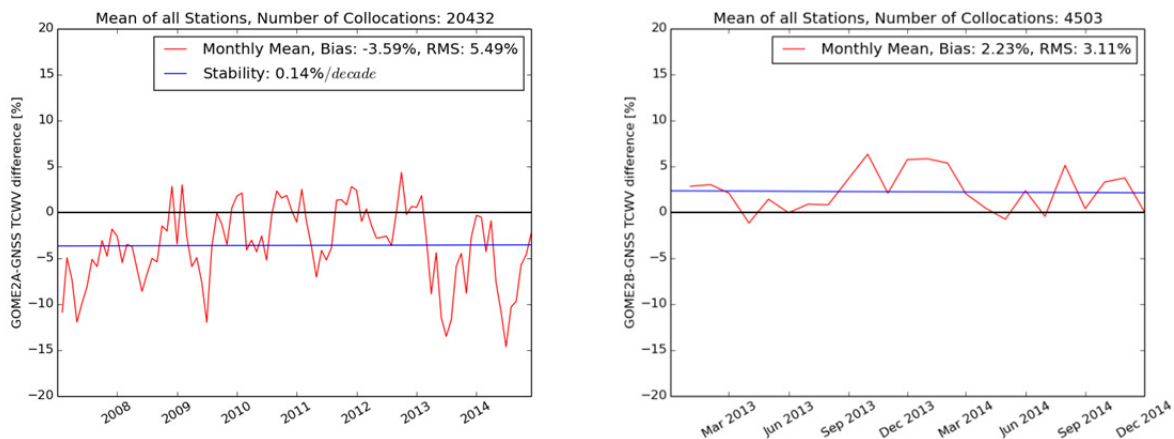

Figure 3-2: Relative Differences from GOME-2A (left) and GOME-2B (right).

Doc:	SAF/AC/DLR/VR/L3_H2O			
Date:	06 November 2017			
Issue:	1	Revision:	1	Page 37

EUMETSAT
AC SAF
ATMOSPHERIC COMPOSITION
MONITORING

3.2 General investigation of GOME-2 vs GNSS

GOME-2A and GOME-2B reveal reasonable agreement with GNSS data. The bias is ±0.5 kg/m² while the RMS is between 4.69 and 5.48 kg/m². Note that point-2-area uncertainties contribute to the RMS and that the temporal sampling is largely different which introduces uncertainty as well. In relative values the bias of GOME-2A is -2.98%, the RMS is 25.40%. GOME-2B has a relative bias of 2.17%, the relative RMS is 29.31%.

The difference in bias between GOME-2A and GOME-2B is relatively large with 0.96 kg/m^2 and 5.15%. This difference will become relevant if the data record exceeds a length of interest for climate analysis.
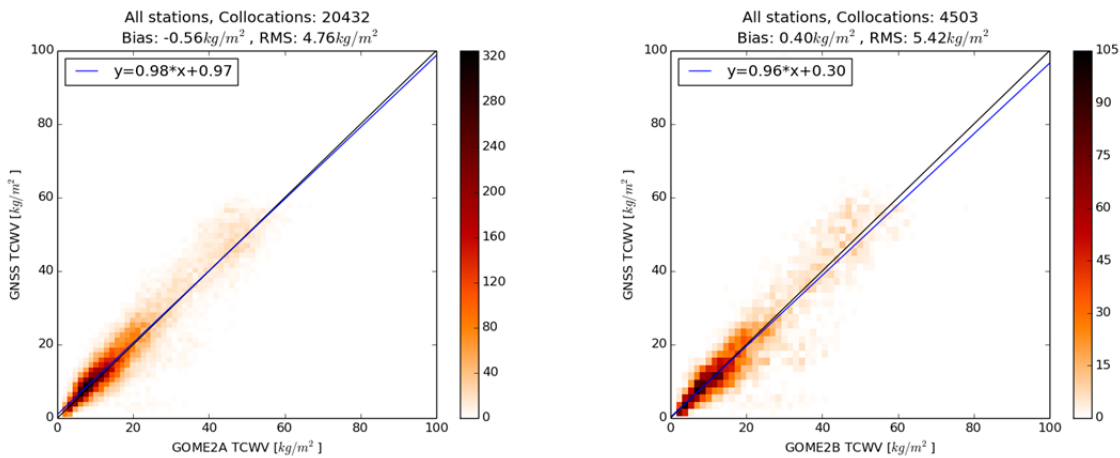

Figure 3-3: Scatter plots of TCWV from GOME-2A (left) and GOME-2B (right) relative to TCWV from GNSS.

3.3 Seasonal investigation

The seasonal investigation is carried out for GOME-2A and GOME-2B and associated results can be found in figure 3-4 and figure 3-5, respectively. The discussion focuses on results shown in figure 3-4.

The absolute largest bias and RMS occur in summer. The bias closest to 0 kg/m^2 is found in fall and the smallest RMS in winter. The RMS exhibits a seasonal cycle with maximum/minimum values in summer/winter. This is expected in view of larger variability associated with larger TCWV values in combination with the annual cycle of TCWV and the misbalance between number of stations in the northern and southern hemispheres [RD-4].

Results for GOME-2B are similar but suffer from low numbers of collocations.
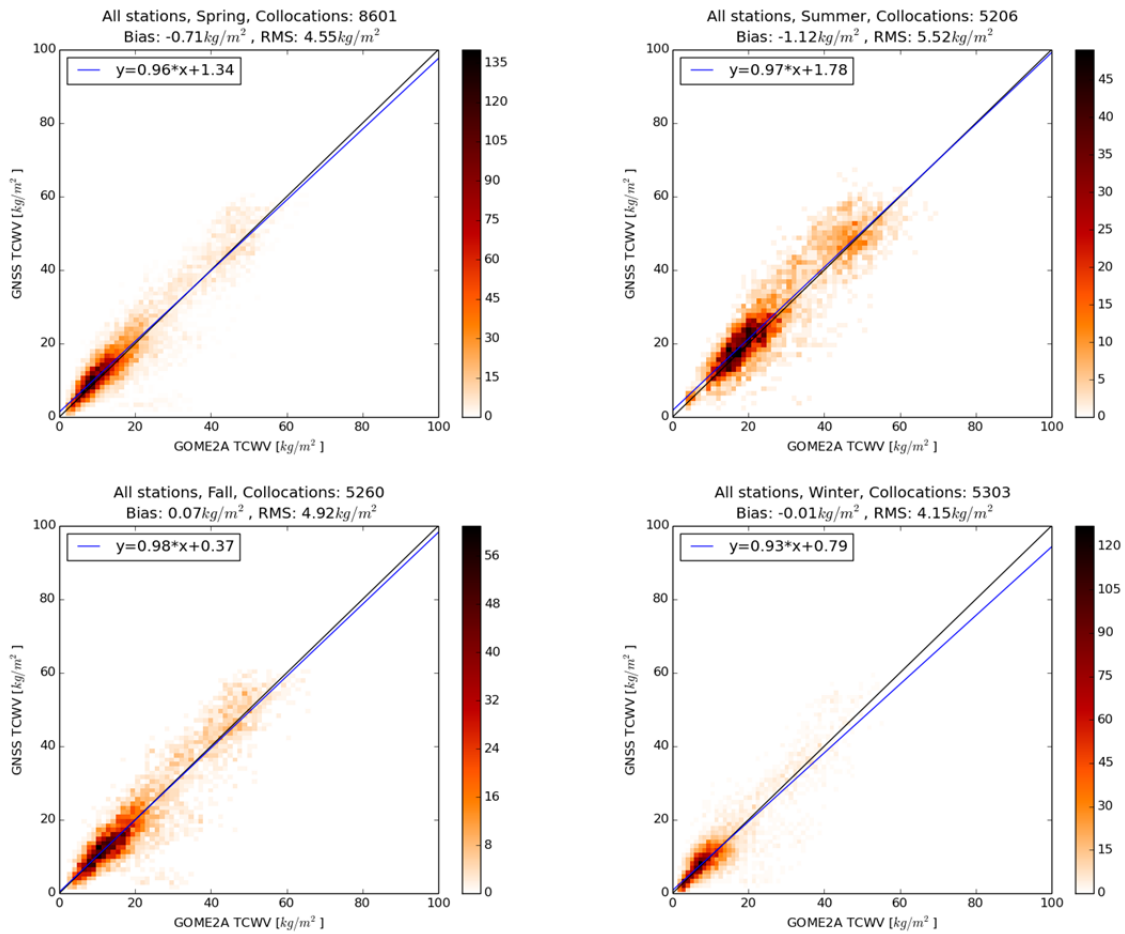
Figure 3-4: Scatter plots of TCWV from GOME-2A and GNSS in case of spring (upper left), summer (upper right), fall (lower left) and winter (lower right).
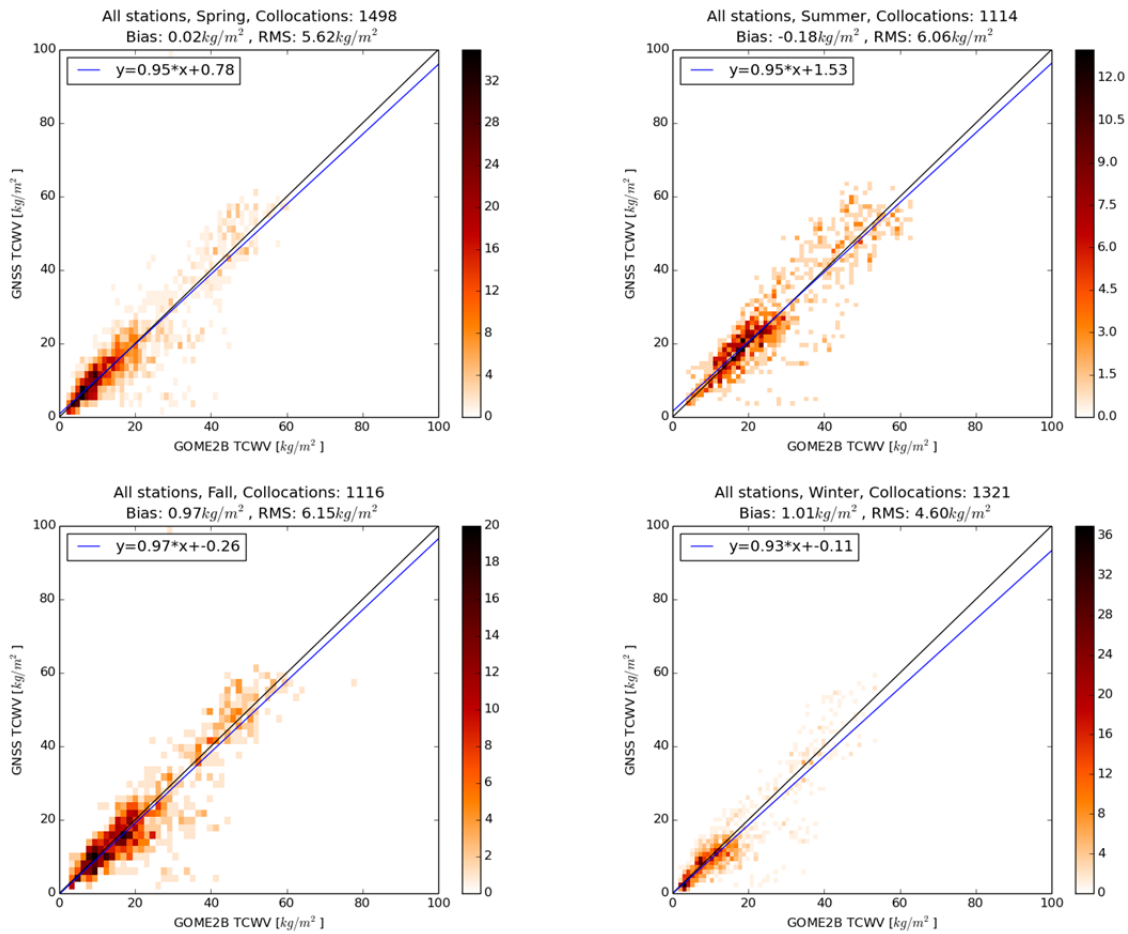
	Doc:	SAF/AC/DLR/VR/L3_H2O			
	Date:	06 November 2017			
	Issue:	1	**Revision:**	1	**Page 39**

EUMETSAT
AC SAF
ATMOSPHERIC COMPOSITION
MONITORING

Figure 3-5: Scatter plots of TCWV from GOME-2B and GNSS in case of spring (upper left), summer (upper right), fall (lower left) and winter (lower right).

Doc:	SAF/AC/DLR/VR/L3_H2O				
Date:	06 November 2017				
Issue:	1	**Revision:**	1		**Page 40**

EUMETSAT
AC SAF
ATMOSPHERIC COMPOSITION
MONITORING

3.4 Global distribution of bias and RMS

Bias and RMS are displayed in figures 3-6 and 3-7 in absolute and relative values, respectively. The results appear mostly random, except for a zonal dependence in case of the absolute RMS. Also, a slight tendency to larger bias and RMS at coastal stations and in the tropics and subtropics is visible.
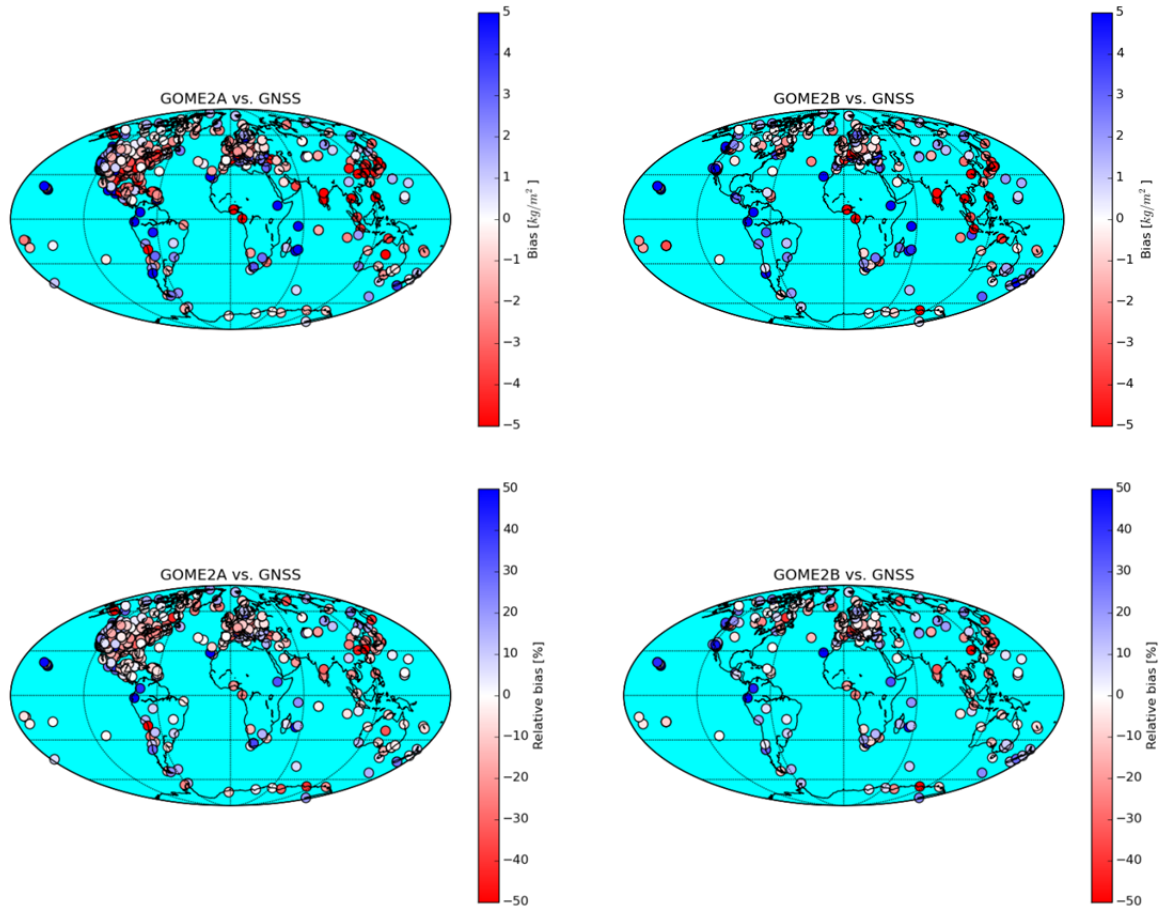

Figure 3-6: Global distribution of the bias by comparing GOME-2A (left) and GOME-2B (right) to GNSS, in absolute (top) and relative (bottom) values.
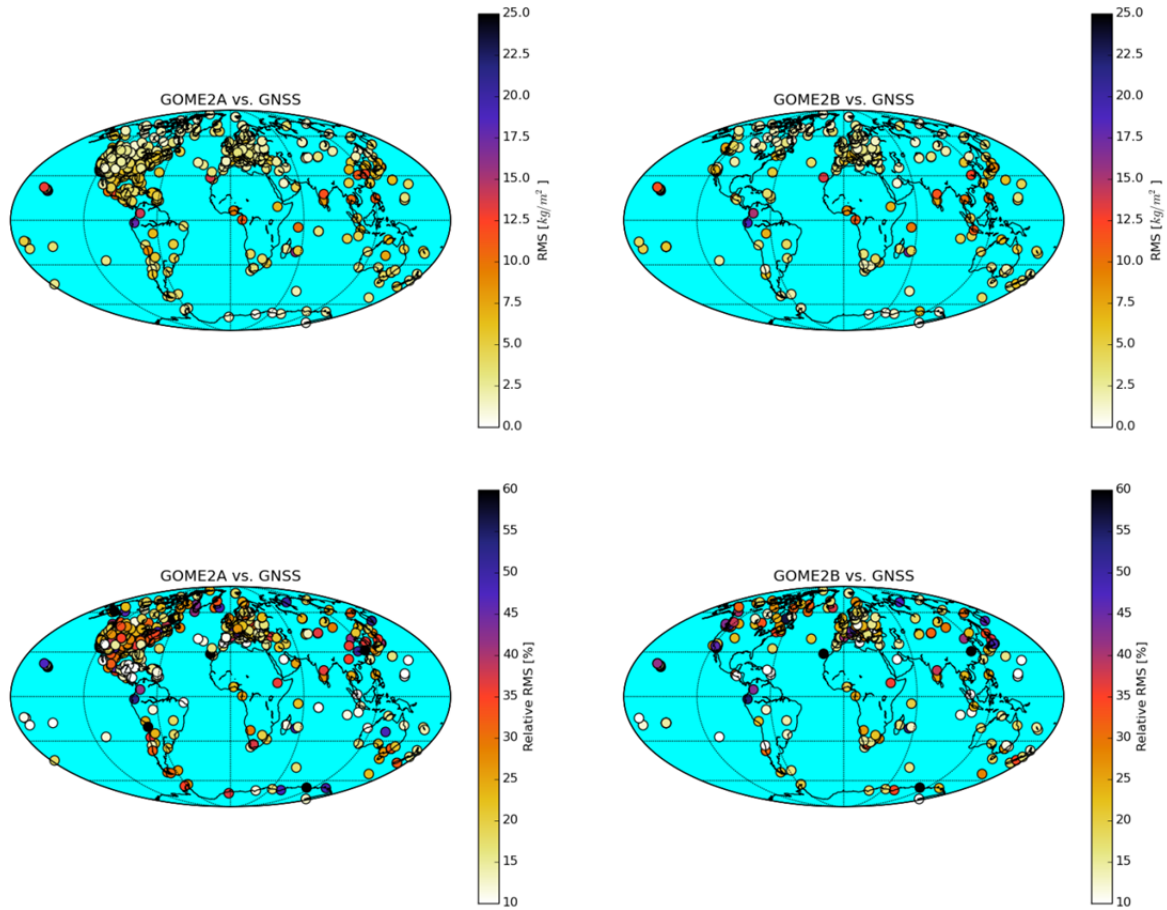
Figure 3-7: Global distribution of RMS by comparing GOME-2A (left) and GOME-2B (right) to GNSS, in absolute (top) and relative (bottom) values.

4. GOME-2 vs GRUAN

The GRUAN version 2 data record contains observations from 11 stations. We thus focus on the general investigation of bias and RMS. A seasonal investigation is not useful for the comparison to GRUAN, since the number of collocations is too small (e.g. only 18 spring collocations for GOME-2B). Nevertheless it should be mentioned that the seasonal investigation supports the features found by the comparison with GNSS. The noise level in the stability analysis is large due to the small number of valid collocations and thus does also not allow conclusions on the stability in this case.

4.1 General investigation of GOME-2 vs GRUAN

Figure 4-1 shows scatter plots of TCWV from GOME-2A and GOME-2B versus GRUAN. Compared to GRUAN, the absolute bias of GOME-2A is larger than the bias of GOME-2B while the RMS is lower. The bias is negative in both cases. The relative bias for GOME-2A is -1.72 kg/m^2 (-9.45%), the relative RMS is 4.23 kg/m^2 (23.4%). In case of GOME-2B the relative bias is -0.70 kg/m^2 (-3.49%), the relative RMS is 5.49 kg/m^2 (27.37%). The difference in bias between GOME-2A and GOME-2B is similar as for the comparison to GNSS, however, at smaller individual bias values. The RMS is similar for GOME-2B and slightly smaller for GOME-2A.
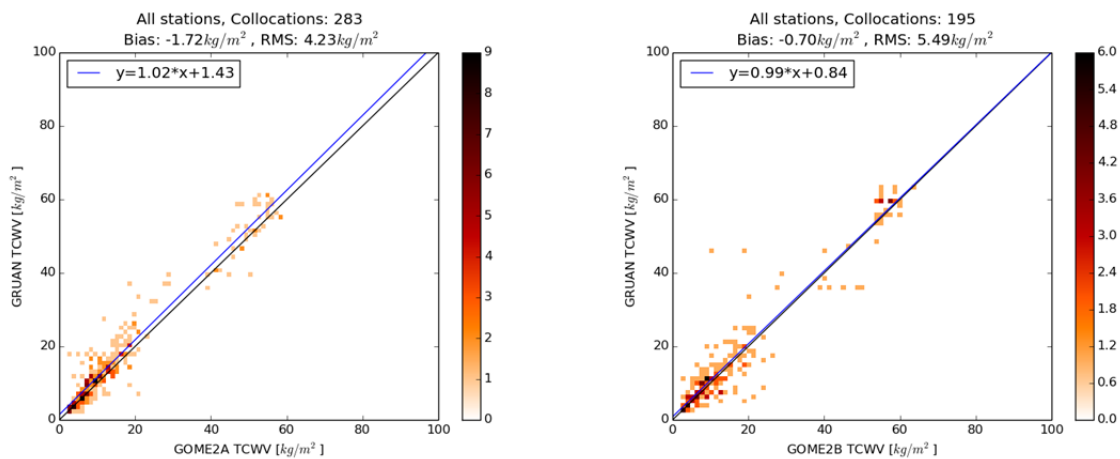

Figure 4-1: Scatter plot of TCWV from GOME-2A (left) and GOME-2B (right) relative to TCWV from GRUAN.

Note that the temporal coverage and resolution of GRUAN data is a function of station, in particular in the early years where data density is low.

5. Conclusions

This report provides a comparison of the GOME-2 monthly mean TCWV data with GNSS and GRUAN monthly averaged TCWV as reference.

The comparison with GNSS reveals the bias to be lower than ± 0.5 kg/m² while the RMS is lower than 5.5 kg/m². The seasonal analysis exhibits that the absolute bias is largest/smallest in summer/fall. The RMS exhibits a seasonal cycle with maximum/minimum values in summer/winter. The global distribution of bias and RMS appears mainly random, except from larger values at coastal stations and a slight tendency for larger values in the tropics (bias and RMS) and a slight zonal dependence (RMS).

Results related to the use of GRUAN data as reference supports the features found in the comparison with GNSS. However, comparing GOME-2 to GRUAN reveals a negative bias for GOME-2A and for GOME-2B, with a comparable difference in bias between the two satellites though. Note that less data was included and therefore some investigations done for GNSS are not adequate for a comparison with GRUAN and are not shown here.

In conclusion a reasonable quality of the GOME-2 products relative to GNSS is observed. However, a break between GOME-2A and GOME-2B seems to be evident. This break has a strength of almost 1 kg/m².

The overall results are summarised in table 5-1.

Table 5-1: Overview of bias and RMS for all investigated cases.

GOME-2	Reference Data	Season	Bias [kg/m²]	RMS [kg/m²]	Number of Collocations
A	GNSS	All	-0.56	4.76	20432
A	GRUAN	All	-1.72	4.23	283
B	GNSS	All	0.40	5.42	4503
B	GRUAN	All	-0.70	5.49	195
A	GNSS	Spring	-0.71	4.55	8601
A	GNSS	Summer	-1.12	5.52	5206
A	GNSS	Fall	0.07	4.92	5260
A	GNSS	Winter	-0.01	4.15	5303
B	GNSS	Spring	0.02	5.62	1498
B	GNSS	Summer	-0.18	6.06	1114
B	GNSS	Fall	0.97	6.15	1116
B	GNSS	Winter	1.01	4.60	1321

6. Acknowledgement